AUTHOR'S COPY.

IN -1443

File as → IN-1443

NASA CR-72781

# SPHERICAL GAS CORE REACTOR CRITICAL EXPERIMENT

Get DRA

J H Lofthouse and J F Kunze

FACILITY FORM 602

N71-34598 (ACCESSION NUMBER)

(THRU)

80 (PAGES)

G3 (CODE)

CR-72781 (NASA CR OR TMX OR AD NUMBER)

22 (CATEGORY)

Prepared for

NATIONAL AERONAUTICS AND SPACE ADMINISTRATION

Contract C-67747-A

Date Published—February 1971

AUG 1971
RECEIVED
NASA STI FACILITY
INPUT BRANCH

IDAHO NUCLEAR CORPORATION

National Reactor Testing Station
Idaho Falls, Idaho

LEGAL NOTICE

This report was prepared as an account of work sponsored by the United States Government Neither the United States nor the United States Atomic Energy Commission, nor any of their employees, nor any of their contractors, subcontractors, or their employees, makes any warranty, express or implied, or assumes any legal liability or responsibility for the accuracy, completeness or usefulness of any information, apparatus, product or process disclosed, or represents that its use would not infringe privately owned rights

IN-1443 Limited Distribution

# S P H E R I C A L  G A S  C O R E  R E A C T O R

# C R I T I C A L  E X P E R I M E N T

by

J H Lofthouse and J F Kunze

Prepared for

NATIONAL AERONAUTICS AND SPACE ADMINISTRATION
Contract C-67747-A

Technical Management
NASA-Lewis Research Center
Cleveland, Ohio

Nuclear Systems Division
Robert E. Hyland, Project Manager

Space Nuclear Propulsion Office
Capt C E Franklin, USAF

IDAHO NUCLEAR CORPORATION

A Jointly Owned Subsidiary of

AEROJET GENERAL CORPORATION
ALLIED CHEMICAL CORPORATION
PHILLIPS PETROLEUM COMPANY

Date Published — February 1971

PREPARED FOR THE U S ATOMIC ENERGY COMMISSION
IDAHO OPERATIONS OFFICE
UNDER CONTRACT NO AT(10-1)-1230

## ABSTRACT

Criticality experiments using gaseous fuel are reported on The experiments were relatively "clean" and should serve as benchmarks for calculational purposes The inner spherical gaseous fuel region (127 cm dia) was located in a 183 cm diameter cavity surrounded by 91 cm of commercial grade heavy water The critical mass was 8 4 kg of uranium in gaseous $UF_6$ form The second configuration had hydrogen added between the fuel and the cavity wall The third added structural material to the cavity wall The critical mass increased to 12 86 kg and 29 2 kg of uranium, respectively Four methods of controlling reactivity were examined Results were favorable, with total control system worths as high as 18 dollars



## ACKNOWLEDGEMENTS

The authors wish to acknowledge the efforts of C G Cooper, R R Jones, and D H Suckling in the operation of the experiment, and of Mrs P L Chase in assisting with data reduction and report preparation Also, credit is given to D A Pearson for his contribution of the neutron spectrum measurements

CONTENTS


| | | |
|---|---|---|
| ABSTRACT | | ii |
| ACKNOWLEDGEMENTS | | ii |
| 1 0 | SUMMARY | 1 |
| 2 0 | INTRODUCTION | 2 |
| 3 0 | DESCRIPTION OF THE TEST ASSEMBLY AND TEST PROCEDURES | 3 |
| | 3 1 Test Assembly | 3 |
| | 3 2 Fuel Transfer and Core Heating System | 4 |
| | 3 3 Test Procedures | 4 |
| 4 0 | CONFIGURATION #1 (Initial Configuration) | 12 |
| | 4.1 Initial Fuel Loading | 12 |
| | 4.2 Reactivity Measurements | 12 |
| | 4 2 1 Control Rod Worth Measurements | 12 |
| | 4 2 2 Material Reactivity Worth Measurements | 13 |
| | 4 3 Power and Flux Distribution Measurements | 14 |
| | 4 3 1 Catcher Foil Data | 14 |
| | 4 3 2 Resonance Foil Detector Data - Gold, Indium and Manganese | 15 |
| 5.0 | CONFIGURATION #2 (Hydrogen Propellent Mockup in Cavity Region) | 28 |
| | 5 1 Fuel and Coolant Mockup Reactivity Worths | 28 |
| | 5 2 Power and Flux Distribution Measurements | 29 |
| 6 0 | CONFIGURATION #3 (Stainless Steel Cavity Liner) | 35 |
| | 6.1 Reactivity and Material Worth Measurements | 35 |
| | 6 2 Power and Flux Distribution Measurements | 36 |
| | 6 2 1 Catcher Foil Data | 36 |
| | 6 2 2 Resonance Foil Detector Data - Gold, Indium and Manganese | 36 |

7 0 CONTROL SYSTEMS EVALUATIONS 47

7 1 Designs 47

7 2 Measurement Method 47

7 3 Results of Pulsed Neutron Data 48

8 0 ANALYTICAL CALCULATIONS 54

9 0 DISUCSSION OF EXPERIMENT AND RESULTS 57

10 0 CONCLUSIONS AND RECOMMENDATIONS 67

APPENDIX A 68

REFERENCES 70

INDEX 72

TABLES


| | | |
|---|---|---|
| 3 1 | Spherical Cavity Reactor Configuration Code | 6 |
| 3 2 | Reactor Component Description | 7 |
| 3 3 | Effective Delayed Neutron Parameters | 9 |
| 4 1 | Nuclear Model of Gas Core Experiment | 16 |
| 4 2 | Initial Loading - Inverse Multiplication | 17 |
| 4 3 | Control Rod Worth Measurements | 19 |
| 4 4 | Catcher Foil Cadmium Ratio - Configuration #1 | 20 |
| 4 5 | Infinitely Dilute Gold Foil Cadmium Ratios and Thermal Flux - Configuration #1 | 21 |
| 4 6 | Infinitely Dilute Indium Foil Cadmium Ratios and Thermal Flux - Configuration #1 | 22 |
| 4 7 | Infinitely Dilute Manganese Foil Cadmium Ratios and Thermal Flux - Configuration #1 | 22 |
| 5 1 | Catcher Foil Cadmium Ratio - Configuration #2 | 30 |
| 5 2 | Infinitely Dilute Gold Foil Cadmium Ratios and Thermal Flux - Configuration #2 | 31 |
| 6 1 | Catcher Foil Cadmium Ratio - Configuration #3 | 38 |
| 6 2 | Infinitely Dilute Gold Foil Cadmium Ratios and Thermal Flux - Configuration #3 | 39 |
| 6 3 | Infinitely Dilute Indium Foil Cadmium Ratios and Thermal Flux - Configuration #3 | 40 |
| 6 4 | Infinitely Dilute Manganese Foil Cadmium Ratios and Thermal Flux - Configuration #3 | 41 |
| 7 1 | Decay Constants for Control Systems | 50 |
| 8 1 | Cross Sections - 19-Energy Group Format | 56 |
| 8 2 | Calculated Eigenvalues for Three Configurations | 56 |
| 9 1 | Summary of Critical Masses and Fuel Worth for Three Configurations | 59 |

FIGURES


| | | |
|---|---|---|
| 3 1 | Overall diagram of the Spherical Cavity Reactor Configuration . | 10 |
| 3 2 | Horizontal cross section showing location of sheet metal shrouds | 11 |
| 4 1 | Inverse multiplication for initial fuel loading of Configuration #1 . | 23 |
| 4 2 | Control system rod worth curves | 24 |
| 4 3 | Relative specific power (U-235 fission rate) in Configuration #1 . | 25 |
| 4 4 | Radial bare gold activity (d/m/gm-watt) in Configuration #1 | 26 |
| 4 5 | Radial gold determined thermal flux-Configuration #1 | 27 |
| 5 1 | Relative specific power (U-235 fission rate) in Configuration #2 | 32 |
| 5 2 | Radial bare gold activity (d/m-gm-watt) in Configuration #2 | 33 |
| 5 3 | Radial gold determined thermal flux-Configuration #2 | 34 |
| 6 1 | Fuel worth vs core loading | 42 |
| 6 2 | Relative specific power (U-235 fission rate) in Configuration #3 | 43 |
| 6 3 | Radial bare gold activity (d/m-gm-watt) in Configuration #3 | 44 |
| 6 4 | Radial gold determined thermal flux in Configuration #3 | 45 |
| 6.5 | Neutron spectrum determined from multiple foils activation . | 46 |
| 7 1 | Control Schemes | 51 |
| 7 2 | Typical detector response plot (all control rods in) | 52 |
| 7 3 | Control worth shape curves | 53 |

9 1 Reactivity changes during heatup and cooldown 60

9 2 Comparison of fuel worth vs fuel loading for two configurations 61

9 3 Comparison of relative radial fission rate for three spherical cavity reactor configurations 62

9 4 Thermal neutron flux determined from bare and cadmium covered gold foils in the sensor well for three configurations 63

9 5 Comparison of neutron spectra calculated from multiple foil exposure and calculated with $S_4$, 19 energy group transport theory (SCAMP code) at a radial distance of 0 0 cm 64

9 6 Comparison of neutron spectra calculated from multiple foil exposure and calculated with $S_4$, 19 energy group, transport theory (SCAMP code) at a radial distance of 61 0 cm 65

9 7 Comparison of neutron spectra calculated from multiple foil exposure and calculated with $S_4$, 19 energy group transport theory (SCAMP code) at a radial distance of 105 0 cm 66

## 1 0 SUMMARY

A spherical gas core critical experiment was conducted in order to provide benchmark results for the cold conditions of a typical nuclear rocket concept This experiment had a significant advantage over previously measured configurations -- it was a relatively clean spherical geometry, and thus could be analyzed by one dimensional reactor physics codes In fact, the perturbations to perfect spherical geometry were experimentally evaluated as being worth less than 3/4%Δk, and thus this experiment can serve as a convenient and "simple" benchmark

The basic reactor dimensions were a core region 127 cm diameter in a cavity 183 cm in diameter and reflected by 91 4 cm of $D_2O$ Three configurations were measured The first, with the bare minimum of structure and no hydrogen in the cavity region, had a critical mass of 8 434 kg of uranium (in the form of 12 52 kg of $UF_6$) When 1 x $10^{21}$ atoms/cc of hydrogen were added to the cavity region between the core and reflector, the critical mass increased to 12 86 kg of U When the cavity wall was made nuclearly thicker by adding 0 019 mean free paths of thermal absorber as 0 076 cm of stainless steel, the critical mass increased to 29 2 kg of U

Efforts were made to correlate these clean (without control systems) spherical experiments using $S_4$ transport theory with 19 energy groups (seven of which were thermal) In these initial efforts, the absolute multiplication factor was calculated to be approximately 1 04, 3%Δk higher than the corrected experimental value The worth of the added stainless steel absorber on the cavity wall was predicted to within approximately 3% However, the worth of adding hydrogen to the cavity was underpredicted by approximately 50% The reason for this discrepancy and of the 3%Δk over prediction of the basic eigenvalue has not been resolved

The commonly proposed methods of controlling this type of reactor is to have movable poison absorber devices in the reflector Four such control schemes were measured using the pulsed neutron generator technique Rotating drums, caps that fit against the cavity wall, and a sleeve that slides down over the cavity wall all yielded very large swings in reactivity These three methods all were worth more than the 23 control rods of the operating control system of the critical experiment Total control system worths exceeding 10%Δk can easily be designed for a gas core system of this type

| | Total Worth %Δk/k | Worth $\frac{\%\Delta k/k}{cm^2}$ |
|---|---|---|
| 23 Control Rods | (3 8 ± 0 4) | |
| 1 Control Drum | (2 0 ± 0 3) | 1 44 x $10^{-3}$ |
| 1 Cap | (3 9 ± 0 5) | 1 58 x $10^{-3}$ |
| 1 Sleeve | (17 ± 4 0) | 96 x $10^{-3}$ |

(Note One dollar = 0 788%Δk)

The concluding reactor run for this series of tests was made at a power of 500 watts for 2 hours duration Nuclear heating was sufficient to maintain the core temperature above 210°F and the external electrical heaters normally used to maintain the $UF_6$ core in the vapor state could be turned off

## 2 0 INTRODUCTION

Over the past several years a continuing series of reactor critical experiments have been performed on a nuclear mockup of a Gas Core Cavity Reactor (ref 1,2,3,4,5) that shows promise for space propulsion applications The work is sponsored by the National Aeronautics and Space Administration, Lewis Research Center and was performed at the Low Power Test Facility at the National Reactor Testing Station in Idaho All of the initial work in the above references was done on a cylindrical configuration Analytical correlation of the test results was difficult and not very extensive because of the exceedingly long convergence time (ref 6) required for either transport or Monte Carlo solutions in two dimensions This, together with the results from recent flowing gas tests (ref 7) showing that a spherical shaped cavity can give large fluid dynamic containment of the gaseous fuel, provided the basis for the spherically shaped experiments

During the latter half of 1969 a spherical geometry Cavity Reactor Mockup was constructed and nuclear testing with a highly enriched $^{235}UF_6$ core commenced This document contains the test data and summarizes the results from the experiment

Following the initial fuel loading to criticality three configurations were tested

Configuration #1 - clean spherical geometry (except for necessary structural material)

Configuration #2 - $1 \times 10^{21}$ atoms/cc hydrogen in the form of styrafoam added to the cavity propellant region, (region between the $UF_6$ sphere wall and the cavity wall)

Configuration #3 - same as Configuration #2 except 0 019 mean free paths of thermal absorber material in the form of stainless steel added to the cavity wall

Throughout this report these three configurations will be referred to as the bare, hydrogen, and stainless steel configurations, respectively.

## 3 0 DESCRIPTION OF THE TEST ASSEMBLY AND TEST PROCEDURES

### 3 1 Test Assembly

Figure 3 1 and Table 3 1 show the arrangement of the reactor system The salient components are labeled and Table 3 2 lists the important component dimensions, weights when known, and construction materials

Concentric spheres, 127 6 cm o d and 183 1 cm o d , respectively with 0 635 cm thick walls nominal, form the core tank and cavity wall The cavity wall sphere composed of two halves is held together with a stainless steel V-band and O-ring seal arrangement Removal of the top hemisphere allows access to the cavity region for installation of test material The cavity wall is also the inner containment for the surrounding heavy water reflector-moderator of the system

The outer containment wall of the reflector-moderator is a tank which provides a minimum $D_2O$ thickness of 91 41 cm (3 feet) This tank consists of a cylindrical section, 365 8 cm (12 feet) in diameter by 152 4 cm (5 feet) in height Truncated conical top and bottom sections are 106 7 cm (3 5 feet) in height and the top and bottom plates forming the ends are 152 4 cm (5 feet) in diameter The tank would thus appear as an octagon in an elevation view and circular in the plan view A portion of the top conical section is a removable lid of sufficient diameter to allow installation and maintenance of the cavity and core spheres Control rod guide tubes (3/4-inch schedule 40 pipe) extend into the $D_2O$ a distance of 86 5 cm from reinforcing plates welded to the side of the tank In addition, a 2-inch schedule 40 pipe extends up from the cavity sphere and serves as a sensor access well to the cavity region and core

The cavity sphere is supported on an 8-inch schedule 40 pipe (o d = 21 91 cm) The core sphere is on a concentric 5-inch schedule 40 pipe with a series of holes through the wall near the core tank The annuli formed by these two columns along with two concentric sheet metal shrouds surrounding the core sphere provide inlet and outlet channels for a forced air heating system to maintain the $UF_6$ fuel in the gaseous state Figure 3 2 shows a horizontal cross section diagram across the core and cavity with nominal dimensions and shroud spacing A 1-inch schedule 40 pipe leading from the fuel transfer and heating system up through the core support column to the core tank provides a means of transferring fuel into and out of the reactor

Control is achieved with eight shim scram actuators, located and equally spaced circumferentially, at the reactor midplane Each actuator, with the exception of one, drives a gang of three poison tips in the control rod guide tubes One guide tube was used as an additional sensor well during power and flux measurements Thus the regular control system consisted of 23 poison tips

## 3.2 Fuel Transfer and Core Heating System

At the start of a normal operation the core tank containing $UF_6$ is heated to vaporize the fuel by drawing air over electrical heaters, through a metal "hot box" and associated ducting leading to the core support column. The hot air then passes up the support column, through some holes through the wall near the top, and out into an annulus formed by the core tank and a thin aluminum shroud open at the top as shown in Figure 3 1 A second, outer, concentric shroud guides the outlet air back to an annulus formed by the core support column and the cavity sphere support column hence out through the exit ducting, which is concentric with the inlet ducting part of the way, to a filter and blower which exhausts the air

Fuel is transferred to the core tank, from a $UF_6$ shipping cylinder heated by the hot air in the "hot box" through a 1-inch schedule 40 pipe which is concentric with the inlet air ducting and core support column A sleeve type valve on the core support column near the top can be adjusted so that the hot air bypasses the core Thus the core tank can be maintained at a temperature sufficiently low to allow condensation of the $UF_6$ vapor being fed into it from the heated cylinder and transfer line with their associated valving

## 3.3 Test Procedures

The principal measurements made on these critical experiments were reactivity, power distributions and flux distribution The achieving of criticality is considered to be only an intermediate step, and though subcritical data can yield information on reactivity, those results are usually less reliable than the measurements made from the critical configuration. When feasible, the measurements were made with the control rods nearly fully withdrawn so as to limit the amount of perturbation of the reflector flux caused by the control rods

Reactivity measurements were made using the delayed neutron parameters, either by means of asymptotic positive period measurements and the inhour equation or by means of the inverse kinetics method of computing reactivity from a flux trace Base conditions were established by measuring the asymptotic period rather than by establishing a level power position The long-lived ($\gamma$-n) reactions in the $D_2O$ created a strong enough spurious neutron source that level power conditions were always subcritical, and by differing amounts depending on the past operating history and hence the strength of the source Period measurements could be made over several decades, thus making possible a reliable extrapolation to the asymptotic, no-source value. The relatively small integrated power of a period measurement also minimized the spurious ($\gamma$-n) source buildup The delayed neutron parameters used for this reactor are given in Table 3 3, and include eight groups of neutrons from ($\gamma$-n) reactions in the heavy water The total delayed fraction (one dollar) was 0 788%*

---

* This value of 0.788% includes corrections for differences in importance of the delayed and prompt neutrons Commonly called the effective $\beta$, this value is slightly higher than the direct $\beta$ because the delayed neutrons are born at a much lower energy

All results are reported in %Δk instead of dollars and cents Without considering uncertainties in the delayed neutron fraction, most period measurements of reactivity have associated with them an uncertainty of approximately ±0 0005%Δk Day-to-day reactivity measurements (at the same average core temperature and constant $D_2O$ reflector temperature) were reproducible to within ±0 0015%Δk Reactivity coefficient measurements made all in the same day (sample vs base) have an approximate uncertainty of no more than ±0.001%Δk.

The temperature coefficient of the core, once all the fuel was vaporized, was too small to be measured over a span of approximately 7°F in the neighborhood of 210°F - i e the temperature coefficient was probably less than 0.0015%Δk per 7°F The reflector temperature coefficient was not measured in this experiment because there was no provision for heating or controlling the temperature of the $D_2O$ However, on an earlier cylindrical configuration (Ref 1, p 172 and 181), the temperature coefficient of the $D_2O$ reflector-moderator was found to be quite significant, approximately -0 014%Δk/°C in the region of 30°C Similar values would be expected for this spherical configuration Day-to-day variations of $D_2O$ temperature were less than 1/2°F From winter to summer the $D_2O$ temperature did vary by 11°F, and thus absolute k-excess values drifted by perhaps as much as 0 08%Δk between the critical condition measurements on Configuration 1 and 3, bare and stainless steel, respectively

In the heating and cooling of the reactor, some unusual effects were observed in reactivity as the fuel was passing to or from the vaporization state These results are discussed in Section 9

Power distribution measurements were routinely made using aluminum fission-product-catcher foils on cleaned uranium metal sheet Reproducibility of results is better than ±2%, and there is no detectable spectral dependence of this technique in the thermal or near thermal range Decay of the foils was automatically included by counting all foils vs a normalizer foil from the same exposure Absolute power levels were determined with a 2π beta counter (3.8 cm radius chamber) precalibrated with absolute fission chambers and gold foils. This counter (an NMC type PC-3) gives 56 fiss/gm of U-235 per count per minute 50 minutes after shutdown from a constant 20 minute exposure. Absolute power levels are believed to be accurate to ±3% standard deviation

Thermal fluxes are reported as equivalent 2200 m/sec fluxes, not as Maxwell-Boltzmann average fluxes The fluxes were determined by use of bare and cadmium covered gold foils The gold was nominally 0.0012 cm thick, with an effective resonance integral of 680 barns (vs 1555 barns infinitely dilute). In computing cadmium ratios, each foil was corrected for its effective resonance integral (ref 8) by its mass to give the infinitely dilute value Thermal flux perturbation was negligible, nominally 2% (ref 9). The cadmium covers employed were 0.05 cm thick, giving an effective cadmium cutoff energy of 0 55 ev (ref. 10)

TABLE 3.1

Spherical Cavity Reactor Configuration Code

| Code No | Description |
|---|---|
| 1 | Core sphere tank |
| 2 | Air flow guide baffles |
| 3 | Cavity sphere tank |
| 4 | Stainless steel V-band connector |
| 5 | $D_2O$ tank |
| 6 | Sensor well |
| 7 | Removable $D_2O$ tank lid |
| 8 | $D_2O$ level sensing and fill level limit switches |
| 9 | Typical of 8 symmetrical control rod actuators and support |
| 10 | Control rod poison tip (cluster of three per actuator) |
| 11 | Control rod guide tube |
| 12 | Core tank support column |
| 13 | Cavity tank support column |
| 14 | $UF_6$ fuel line |
| 15 | Cavity tank hold down rod (typical of 8 symmetrical) |
| 16 | Core tank valve |
| 17 | Air operated $D_2O$ quick dump valve |
| 18 | Motor operated $D_2O$ inlet control valve |
| 19 | $D_2O$ fill line |
| 20 | $D_2O$ pump |
| 21 | $D_2O$ overflow and cover gas return line |
| 22 | Main support column |
| 23 | Valve bellows and valve actuating mechanism |
| 24 | $D_2O$ tank support column |
| 25 | Emergency $D_2O$ catch tank |
| 26 | Work platform |
| 27 | Hand rail |
| 28 | $UF_6$ transfer and core heating system |
| 29 | $D_2O$ storage tank |

TABLE 3 2

Reactor Component Description

| Component | General Description | Weight kg | Dimensions | Material |
|---|---|---|---|---|
| Core tank | Two spun hemispheres welded together. Designed for internal pressure of 50 psig at 230° F. | 90 72 | 127.55 cm O.D. x 0.635 cm wall nominal | 5052 Al |
| Core tank sensor well flange | 2-inch pipe flange and neck extends above core tank 12 86 cm | 2 (calc.) | | 6061 Al |
| $UF_6$ inlet line | 1-inch schedule 40 pipe | | 3 34 cm O D x 0 338 cm wall | 5052 Al |
| Core tank support column | 5-inch schedule 40 pipe | | 14 12 cm wall x 0 655 cm wall | 5052 Al |
| Cavity tank wall | Two spun hemispheres held together with a SS V-band clamp and sealed with a butyl rubber O-ring | 170.1 | 183 10 cm O.D x 0 635 cm wall nominal | 5052 Al |
| Cavity tank support column | 8-inch schedule 40 pipe | | 21 9 cm O D x 0 818 cm wall | 5052 Al |
| V band connecter and bolts | Marmon V-band clamp | 8 62 | | 301 SS |
| Sensor well guide tube | 2-inch schedule 40 pipe | | | 1100 Al |

TABLE 3 2

(Continued)

| Component | General Description | Weight kg | Dimensions | Material |
|---|---|---|---|---|
| Control rod guide tubes | 3/4-inch schedule 40 pipe sealed at one end with welded flat plate | | | 5086 Al |
| Control rod guide tube end spacers | Triangular piece - one on the end of each gang of 3 guide tubes | 325 ea. | | 1100 Al |
| Startup neutron source guide tube | 1 1/2-inch schedule 40 pipe - penetrates reflector-moderator tank above midplane and extends downward at 30° angle to cavity tank wall near midplane | | | 5052 Al |
| Cavity tank hold down rods | 8 - 9/16-inch diam. rods equally spaced around periphery of cavity tank and extending downward to the floor of the reflector moderator tank | | | 6061 Al |
| Air flow circulation baffles | 2 concentric octagonal spheres with a transition to cylindrical at the bottom- constructed from 20 gauge aluminum sheet | 29.94 | | 1100 Al |
| Core tank valve push rod | 1/2-inch diameter rod | | | 1100 Al |

TABLE 3 3

Effective Delayed Neutron Parameters

| Group | $\beta_i$ | $\lambda_i$ |
|---|---|---|
| 1 | 0 000217 | 0 012400 |
| 2 | 0.001460 | 0 030500 |
| 3 | 0 001315 | 0 111000 |
| 4 | 0 002640 | 0 301000 |
| 5 | 0 000766 | 1 100000 |
| 6 | 0.000280 | 3 000000 |
| 7 | 0 000780 | 0.277000 |
| 8 | 0 000240 | 0 016900 |
| 9 | 0 000084 | 0 004810 |
| 10 | 0 000040 | 0 001500 |
| 11 | 0 000025 | 0 000428 |
| 12 | 0 000028 | 0.000117 |
| 13 | 0 000004 | 0 000044 |
| 14 | 0 000001 | 0 000004 |
| | 0 007652 | |

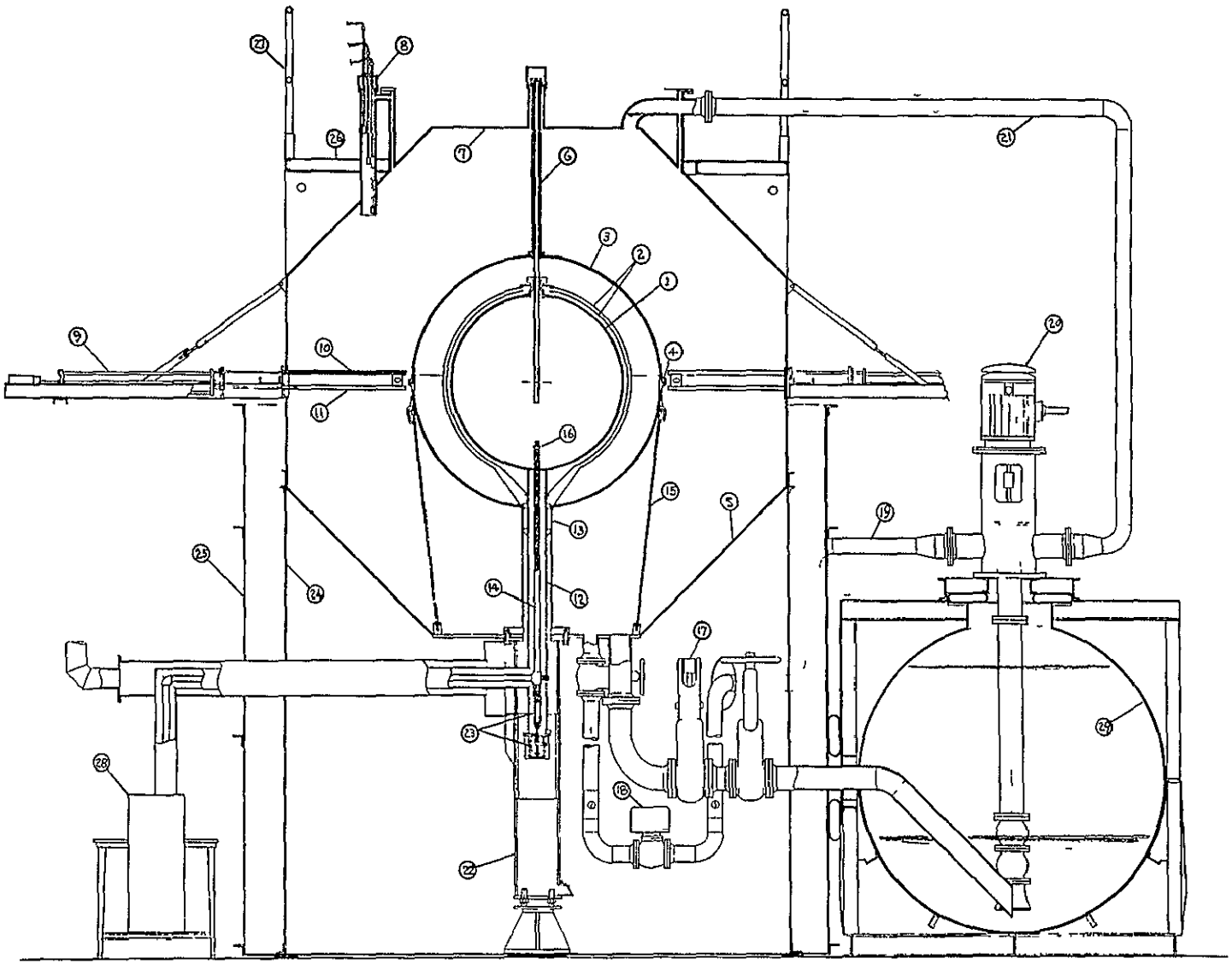

Fig. 3.1 Overall diagram of the Spherical Cavity Reactor Configuration

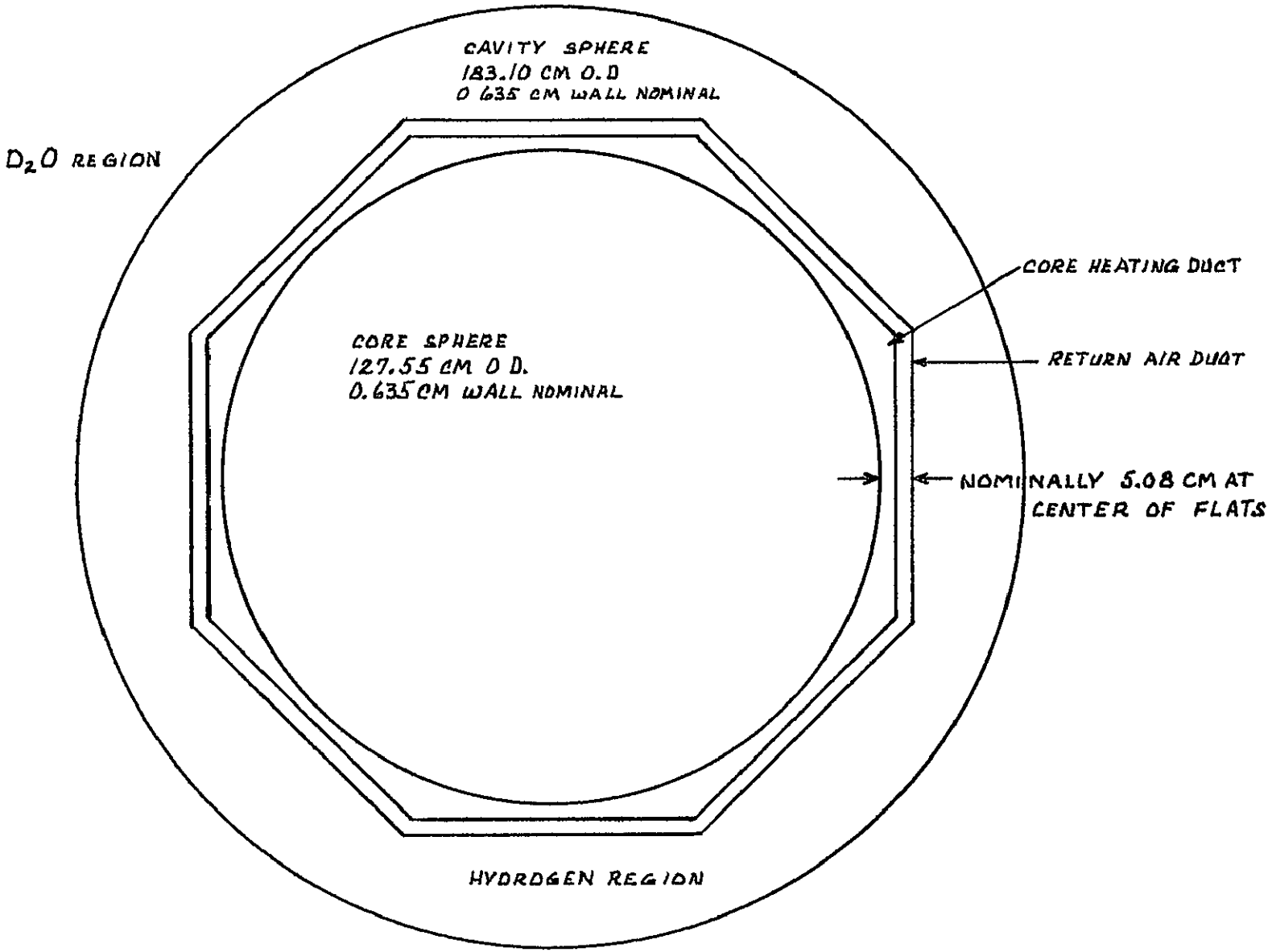


Fig 3 2 Horizontal cross section showing location of sheet metal shrouds

## 4.0 CONFIGURATION #1 (Initial Configuration)

### 4 1 Initial Fuel Loading

Initial $UF_6$ transfer to the core tank and the taking of inverse multiplication data began on December 4, 1969 Prior to any actual fuel loading a 19-group transport calculation was performed with the SCAMP (ref. 11) Code to estimate the critical mass The calculation with a slight adjustment from fuel worth measurements made on previous configurations (Figure 3 3, Ref 3) resulted in calculated critical uranium mass of 8 4 kilograms The actual adjusted critical loading completed on December 10, 1969, was 8 434 kilograms uranium The mathematical spherical model used for the calculation is given in Table 4.1

A normal incremental loading procedure was followed Three counting channels were used to monitor multiplication After the tenth increment with a fuel loading of 8 673 kilograms of uranium (12 880 kilograms $UF_6$) the reactor was critical with a k-excess of 0 2404%$\Delta k/k$ Loading and counting data is given in Table 4 2 and the average inverse multiplication from the three counting channels is plotted in Figure 4 1

### 4.2 Reactivity Measurements

#### 4.2.1 Control Rod Worth Measurements

The reactivity worth of two of the eight control rods (actuators 4 and 8) was measured by period measurements and the data are tabulated in Table 4 3 In addition, a single rod (actuator 4) and an all rods insertion flux trace was obtained from the critical position, from which the rod worth shape curve was obtained by an inverse kinetics calculation The rod shape from these calculations along with the points obtained by the period measurements are shown in Figure 4 2. The total rod worth of actuator #4 by inverse kinetics was (0.62±0 04)%$\Delta k$ By period measurement of incremental sections, actuator #4 is worth 0 585%$\Delta k/k$ and actuator #8 is worth 0 534%$\Delta k/k$ Actuators 4 and 8 are 180° apart around the $D_2O$ tank When the worth difference was observed from the measurements an inspection of geometry revealed that the cavity sphere is slightly off center (by ~ 1 cm) with respect to the ring of actuators and that the tips of actuator #4 in the inserted position are slightly closer to the cavity wall than those of actuator #8, which accounts for the difference in worth Fortuitously, these two actuators are located at the points of greatest offset of the cavity sphere, therefore the total control system worth was estimated to be eight times the average worths of actuators #4 and #8 or 4.289%$\Delta k/k$ (adjusted for one poison tip missing from actuator #5 where the guide tube was used as a sensor well into the $D_2O$) This total control system worth is probably slightly high, since it assumes no "shadowing-interaction" of actuator worths This effect is at most 2 to 3% of the total summed worth, which was the limiting accuracy of the measurements that attempted to evaluate the interaction effects

4.2 2 Material Reactivity Worth Measurements

Fuel worth in the core was determined by adding a 197 67 gm increment of $UF_6$ to the initial fuel loading $UF_6$ worth is 1 99%Δk/k per kilogram of the hexafluoride or 2 96%Δk/k per kilogram of highly enriched uranium (93 2%$U^{235}$) metal

The functional loss of a valve isolating the core tank from the fuel transfer line made it necessary to make all measurements with fuel in the transfer line To evaluate the worth of fuel in the line, a mockup of the line, through the $D_2O$ and cavity, was constructed by wrapping sheet fuel on an aluminum wand and measuring the worth of the mockup in the sensor well The 27 5 grams of sheet fuel (oralloy), at evenly spaced intervals along the wand to simulate a uniform radial distribution, was worth 3 833%Δk/k on a per kilogram basis

The results of the two foregoing measurements were used to correct the initial loading for comparison to the clean calculated critical mass value spoken of in 4 1 above

One additional fuel worth measurement was made in the sensor well with sheet fuel by placing 6 94 grams of oralloy, evenly distributed on a wand over a 22 8 cm length of the core radius from the center This fuel was worth 1 50%Δk/k on a per kilogram basis, and is approximately a core-center fuel worth.

Stainless steel worth on the cavity wall was evaluated by placing 934 grams (4 strips) of type 304 on the $D_2O$ side of the wall. This measurement yielded a value of -0.2547%Δk/k per kilogram If this worth is applied to the stainless steel V-band connector holding the two hemispheres of the cavity tank together to create the seal then the reactivity worth of the V band (8 62 kg) is -2.20%Δk/k

One additional stainless steel measurement was made to evaluate the worth of four stainless steel bolts used to fasten the flange containing the sensor well to the top flange of the core tank This measurement was made by placing an identical bolt (142 2 grams) in the sensor well at the same radial position as the flange bolts From the measurement the four flange bolts were calculated to be worth -0 105%k/k.

To evaluate the worth of the aluminum in the support columns to the core and cavity tanks and of the void they create through the $D_2O$ an aluminum mockup tank was constructed It was installed at the top of the reactor around the sensor well tube through the $D_2O$ The reactivity worth of this tank was -0 541%Δk/k. The worth of a 21 6 cm (8.5 inches) length of aluminum pipe (5-inch schedule 40) in the void between cavity wall and the outer air baffle around the core tank was worth -0.0637%Δk/k. If a linear extrapolation of this worth to a pipe 30 5 cm in length is made and added to the worth of the mockup in the $D_2O$ then the worth of the support pipes and the void created in the $D_2O$ is worth -0 631%Δk/k.

The worth of aluminum on the core tank wall was measured as -0 0410%Δk/k per kilogram by placing 3 36 kilograms of type 1100 aluminum strips between the tank wall and the inner air baffle shroud This is about double the worth in the cylindrical geometry at edge of core (ref. 3, p 45)

Using the applicable material worths above applied to the mass of the structural material in the assembly the following reactivity worths were calculated

| | %Δk/k |
|---|---|
| Al Core wall | -3 72 |
| Air guide shrouds | -1 23 |
| *Support columns & void | -0 631 |
| *Fuel in transfer line | +0 033 |
| *SS bolts in core flange | -0 105 |
| SS V-band connector | -2 20 |
| Al core flange | -0 344 |
| Al cavity wall | -8 36 |

Those items with an asterisk in front perturb the spherical one-dimensional uniformity of the system and therefore cannot be correctly (and easily) incorporated into a spherical reactor model The other items in the above list have essentially spherical symmetry and can be included in a calculational model

In preparation for going to a new configuration with CH and $CH_2$ in the cavity region to mock up a hydrogen propellent, a cylindrical lump of 193 gms of polyethelene(rolled sheet to form a cylinder 5 1 cm diameter by 15 24 cm long) was installed in the sensor well so that it extended from the cavity wall to the core sphere sensor well flange (0 56 of the distance between the cavity wall and the outside of the core sphere) The reactivity worth was measured as -0 140%Δk/k per kilogram

## 4 3 Power and Flux Distribution Measurements

Power and flux distributions over the radius of the reactor were determined in both the sensor well and a rod guide tube by exposing both bare and cadmium covered catcher foils, gold foils, indium foils and manganese foils In addition, cadmium ratios and thermal flux were calculated from the data taken at selected points All cadmium covered foils were enclosed in 0.051 cm (20 mil) thick buckets The method used to calculate the infinitely dilute cadmium ratios and thermal flux are given in Appendix 1

### 4 3 1 Catcher Foil Data

Catcher foil data are plotted as a fine radial power distribution relative to the power at the core center in Figure 4 3 and the cadmium ratio, which is the ratio of the normalized counts from bare and cadmium covered foils exposed at selected radial positions, are given in Table 4 4 Because of the short range of the fission products in the uranium metal foils, these cadmium ratios are essentially infinitely dilute values Therefore, they represent the ratio of total to epithermal fission rate

### 4.3.2 Resonance Foil Detector Data - Gold, Indium and Manganese

Figure 4 4 is a plot of radial bare gold activity distribution, of $1.2 \times 10^{-3}$ cm thick gold The actual response of foils of this thickness to thermal and epithermal neutrons can be determined by comparing columns 2 and 4 of Table 4 5. However, for general usefulness, the infinitely dilute response of total to epithermal neutrons is preferred, and this is given in column 6 of that table Bare and cadmium covered gold, indium and manganese foils were exposed at selected radial locations in both the sensor well and a rod guide tube. The calculated infinitely dilute cadmium ratios and the thermal flux data are shown in Tables 4 5, 4.6 and 4 7. In addition the thermal flux determined from the gold foil activity is plotted in Figure 4 5 All of the data are normalized to a power of one watt as determined from volume weighted catcher foil activity within the spherical core

TABLE 4 1

Nuclear Model of Gas Core Experiment

| Region | Inner Radius (cm) | Outer Radius (cm) | Materials | Mass (kg) |
|---|---|---|---|---|
| Core | 0.0 | 63.138 | $UF_6$* | to be determined |
| | | | Al (type 1100) | 0.546 |
| Core tank wall | 63.138 | 63.773 | Al (type 5052) | 90 72 |
| "Void" between core & reflector | 63.773 | 90.92 | Al (type 1100) | 29 9 |
| | | | Al (type 5052) | 8 38 |
| | | | SS (type 301) | 661 |
| | | | $UF_6$ | 0 17% core mass |
| Cavity tank wall | 90.92 | 91.555 | Al (type 5052) | 170.1 |
| Moderator Region A (with V-band connector) | 91.55 | 94.095 | Al (type 5052) | 1 5 |
| | | | SS (type 301) | 8 6 |
| | | | Heavy water** | remainder of volume |
| Moderator Region B | 94.095 | 122.035 | Al (type 5052) | 7.71 |
| | | | $D_2O$** | remainder of volume |
| Moderator Region C | 122 035 | 152.515 | Al (type 5052) | 5.11 |
| | | | $D_2O$** | remainder of volume |
| Moderator Region D | 152.515 | 188.14*** | Al (type 5052) | 5 11 |
| | | | $D_2O$** | remainder of volume |

* Isotopic composition is 93.2% $U^{235}$

** (Volume fraction of light water ($H_2O$) was 0 0028±0 0002)

*** Equivalent spherical inside radius to match the volume of the outer tank which consists of a cylinder 152 5 cm high by 366 cm dia and two truncated cones, each approximately 117 cm high by 152 cm dia on the small end

TABLE 4 2

Initial Loading

Inverse Multiplication

| Increment | Total Fuel in Core (kg U) | Channel No. 1 CPM | Channel No. 1 $CR_o/CR$ | Channel No. 2 CPM | Channel No. 2 $CR_o/CR$ | Channel No. 3 CPM | Channel No. 3 $CR_o/CR$ | Average | Rod Positions |
|---|---|---|---|---|---|---|---|---|---|
| 0 | 0 | 625 | 1.000 | 661 | 1 000 | 681 | 1 000 | 1 000 | In |
| ($CR_o$) | 0 | 814 | 1.000 | 904 | 1.000 | 889 | 1 000 | 1 000 | Out |
| 1 | 1 50 | 1140 | 0 548 | 1171 | 0 565 | 905 | 0 752 | 0 622 | In |
| 1 | 1 50 | 1561 | 0 521 | 1700 | 0 532 | 1233 | 0 721 | 0 591 | Out |
| 2 | 2 17 | 1430 | 0 437 | 1425 | 0 464 | 1323 | 0 515 | 0 472 | In |
| 2 | 2.17 | 1979 | 0 411 | 2100 | 0 430 | 1988 | 0 447 | 0 429 | Out |
| 3 | 3 05 | 1847 | 0.338 | 1860 | 0 355 | 1871 | 0 364 | 0 352 | In |
| 3 | 3.05 | 2682 | 0 304 | 2820 | 0 321 | 2552 | 0 348 | 0 324 | Out |
| 4 | 4.31 | 2472 | 0.253 | 2481 | 0 266 | 2485 | 0.274 | 0 264 | In |
| 4 | 4 31 | 3881 | 0 210 | 4106 | 0 220 | 3740 | 0 238 | 0 223 | Out |
| 5 | 5.83 | 3994 | 0.156 | 3988 | 0.166 | 3752 | 0 182 | 0 168 | In |
| 5 | 5.83 | 7431 | 0 110 | 7782 | 0 166 | 6514 | 0 136 | 0 121 | Out |
| 6 | 6.66 | 5248 | 0 119 | 5338 | 0 124 | 4746 | 0 143 | 0 127 | In |
| 6 | 6.66 | 11626 | 0 070 | 12274 | 0.074 | 9886 | 0 090 | 0.078 | Out |
| 7 | 7.06 | 6218 | 0 101 | 6296 | 0.105 | 5544 | 0 123 | 0 110 | In |
| 7 | 7.06 | 15873 | 0.051 | 16794 | 0 054 | 13271 | 0.067 | 0.057 | Out |
| 8 | 8.06 | 10569 | 0.059 | 10573 | 0.063 | 9300 | 0.073 | 0 065 | In |
| 8 | 8.06 | 96096 | 0 0085 | 104749 | 0.0086 | 76467 | 0 0116 | 0 0096 | Out |

TABLE 4.2

(Continued)

Inverse Multiplication

| Increment | Total Fuel in Core (kg U) | Channel No. 1 CPM | Channel No. 1 $CR_o/CR$ | Channel No. 2 CPM | Channel No. 2 $CR_o/CR$ | Channel No 3 CPM | Channel No 3 $CR_o/CR$ | Average | Rod Positions |
|---|---|---|---|---|---|---|---|---|---|
| 9 | 8.16 | 11128 | 0.0562 | 11190 | 0 0591 | 9603 | 0 0710 | 0 0621 | In |
| 9 | 8.16 | 139936 | 0.00582 | 153866 | 0.00588 | 110736 | 0 00803 | 0 00658 | Out |
| 10 | 8.40 | 13185 | 0.0474 | 13166 | 0.0502 | 11316 | 0.0602 | 0 0526 | In |

TABLE 4.3

Control Rod Worth Measurements

| Run Number | Actuator Positions | Actuator #8 Position | Reactivity Worth of Increment %Δk/k |
|---|---|---|---|
| 10 | 1,2,3,5,6,7 out<br>4 at 3813 | in(173) to 1062 | .1631 |
| 9 | 1,2,3,5,6,7 out<br>4 at 2000 | 1063 to 2500 | .1834 |
| 11 | 1,2,3,5,6,7 out<br>4 at 818 | 2500 to 5500 | 1574 |
| 12 | 1,2,3,5,6,7 out<br>4 at 818 | 2500 to 6513 | .1751 |
| 13 | 1,2,3,5,6,7 out<br>4 at 393 | 3500 to 6513 | 0919 |
| 14 | 1,2,3,5,6,7 out<br>4 at 393 | 3500 to out (9613) | .1040 |
| | | Actuator #4 Position | |
| 29 | 1,2,3,5,6,7 out<br>8 at 5382 | in(134) to 700 | 1217 |
| 26 B* | 1,2,3,5,6,7 out<br>8 at 6259 | 700 to 1500 | 1352 |
| 28 B* | 1,2,3,5,6,7 out<br>8 at 4570 | 1500 to 3000 | .1727 |
| 28 C* | 1,2,3,5,6,7 out<br>8 at 2032 | 3000 to out (9553) | 1558 |

* These measurements were made with a different core configuration

TABLE 4 4

Catcher Foil Cadmium Ratio

Configuration #1

| Radius (cm) | Bare Foil Counts | Cadmium Covered Foil Counts | Cadmium Ratio |
|---|---|---|---|
| Sensor Well | | | |
| 20 | 114828 | 5789 | 19 836 |
| 40 | 123464 | 5616 | 21 984 |
| 60 | 147648 | 5806 | 25 430 |
| 90 | 198404 | 6308 | 31 453 |
| 110 | 307806 | 2530 | 121 662 |
| 130 | 217384 | 1660 | 130 954 |
| 150 | 131335 | 290 | 452 879 |
| 170 | 52750 | 154 | 342 532 |
| Guide Tube | | | |
| 110 | 305803 | 2323 | 131 641 |
| 130 | 232745 | 395 | 589 227 |
| 150 | 123726 | 127 | 974 220 |
| 170 | 49859 | 81 | 615 543 |

TABLE 4.5

Infinitely Dilute

Gold Foil Cadmium Ratios and Thermal Flux

Configuration #1

| Radius (cm) | Bare Foil d/m/gm-watt x $10^{-5}$ | Bare Foil wt (g) | Cad Cov. Foil d/m/gm-watt x $10^{-5}$ | Cad Cov. Foil wt (g) | Cadmium Ratio | Thermal Flux n/cm$^2$-sec/watt x $10^{-6}$ |
|---|---|---|---|---|---|---|
| Sensor Well | | | | | | |
| 5 | 2.728 | 0356 | 1.083 | .0355 | 1 661 | 2.554 |
| 25 | 2 871 | .0360 | 1 072 | .0370 | 1.713 | 2 772 |
| 45 | 3 089 | 0346 | 1.079 | .0365 | 1.791 | 3 081 |
| 75 | 3.869 | 0357 | 1 106 | 0361 | 2 077 | 4.278 |
| 105 | 5 274 | 0372 | 0.607 | .0367 | 4 301 | 7.245 |
| 125 | 3.928 | 0363 | 0.091 | 0371 | 19 034 | 5 951 |
| 145 | 2.258 | .0358 | 0.013 | .0328 | 80 859 | 3.484 |
| 185 | 0.138 | 0352 | 0.001 | 0351 | 53 603 | 0.213 |
| Guide Tube | | | | | | |
| 97 5 | 5 098 | 0363 | 1 029 | 0376 | 2.673 | 6.289 |
| 105 | 5 520 | .0365 | 0.706 | 0351 | 3.984 | 7.484 |
| 115 | 4.954 | 0358 | 0 284 | .0358 | 8 138 | 7 245 |
| 125 | 4.048 | .0366 | 0.084 | .0379 | 20 973 | 6.147 |
| 135 | 3.092 | .0350 | 0.026 | 0359 | 52.918 | 4.756 |
| 145 | 2.336 | .0346 | 0 008 | .0359 | 132 875 | 3 612 |
| 155 | 1.605 | .0363 | 0.003 | 0355 | 246 444 | 2.485 |
| 165 | 1.030 | 0375 | 0.002 | 0353 | 267.098 | 1 595 |
| 175 | 0.507 | 0358 | 0.001 | .0360 | 201 362 | 0.785 |
| 185 | 0 105 | 0346 | 0001 | 0363 | 2324 16 | 0.163 |

TABLE 4 6

Infinitely Dilute

Indium Foil Cadmium Ratios and Thermal Flux

Configuration #1

| Radius (cm) | Bare Foil d/m/gm-watt x $10^{-7}$ | Bare Foil wt (g) | Cad. Cov. Foil d/m/gm-watt x $10^{-7}$ | Cad. Cov. Foil wt. (g) | Cadmium Ratio | Thermal Flux n/cm$^2$-sec/watt x $10^{-6}$ |
|---|---|---|---|---|---|---|
| Sensor Well | | | | | | |
| 5 | 5.733 | .00584 | 2.725 | .00515 | 1 808 | 2.569 |
| 60 | 5 217 | .00510 | 2.807 | .00584 | 1.568 | 1.920 |
| 90 | 8.755 | .00518 | 2.522 | 00740 | 2.531 | 4 967 |
| 120 | 8 568 | 00518 | 0.851 | .00519 | 7.442 | 6 409 |
| 170 | 0.403 | .00512 | 0.003 | .00679 | 77.552 | 0 332 |
| 185 | 0.260 | .00649 | 0 0008 | .00562 | 227 497 | 0.215 |
| Guide Tube | | | | | | |
| 120 | 9 244 | .00515 | 0.515 | 00512 | 13 073 | 7.251 |
| 185 | 2.061 | .00516 | 0.0003 | 00510 | 408 227 | 0 171 |

TABLE 4 7

Infinitely Dilute

Manganese Foil Cadmium Ratios and Thermal Flux

Configuration #1

| Radius (cm) | Bare Foil d/m/gm-watt x $10^{-6}$ | Bare Foil wt. (g) | Cad. Cov. Foil d/m/gm-watt x $10^{-5}$ | Cad. Cov. Foil wt. (g) | Cadmium Ratio | Thermal Flux n/cm$^2$-sec/watt x $10^{-6}$ |
|---|---|---|---|---|---|---|
| Sensor Well | | | | | | |
| 5 | 2.022 | .0426 | 1 559 | 0407 | 6.924 | 4.208 |
| 60 | 2.654 | 0415 | 1 548 | 0480 | 8 511 | 5 611 |
| 90 | 3 652 | .0427 | 1.513 | 0459 | 11.958 | 7.876 |
| 120 | 4 639 | .0430 | 0.214 | 0415 | 107.153 | 10 400 |
| 145 | 2.590 | .0456 | 0.024 | .0426 | 534.093 | 5.828 |
| 170 | 0.878 | .0459 | 0 007 | 0467 | 567.595 | 1.975 |
| Guide Tube | | | | | | |
| 97.5 | 4.724 | .0432 | 1.440 | 0430 | 16.422 | 10 320 |
| 170 | 0.913 | .0433 | 0.004 | .0424 | 1075.464 | 2 055 |

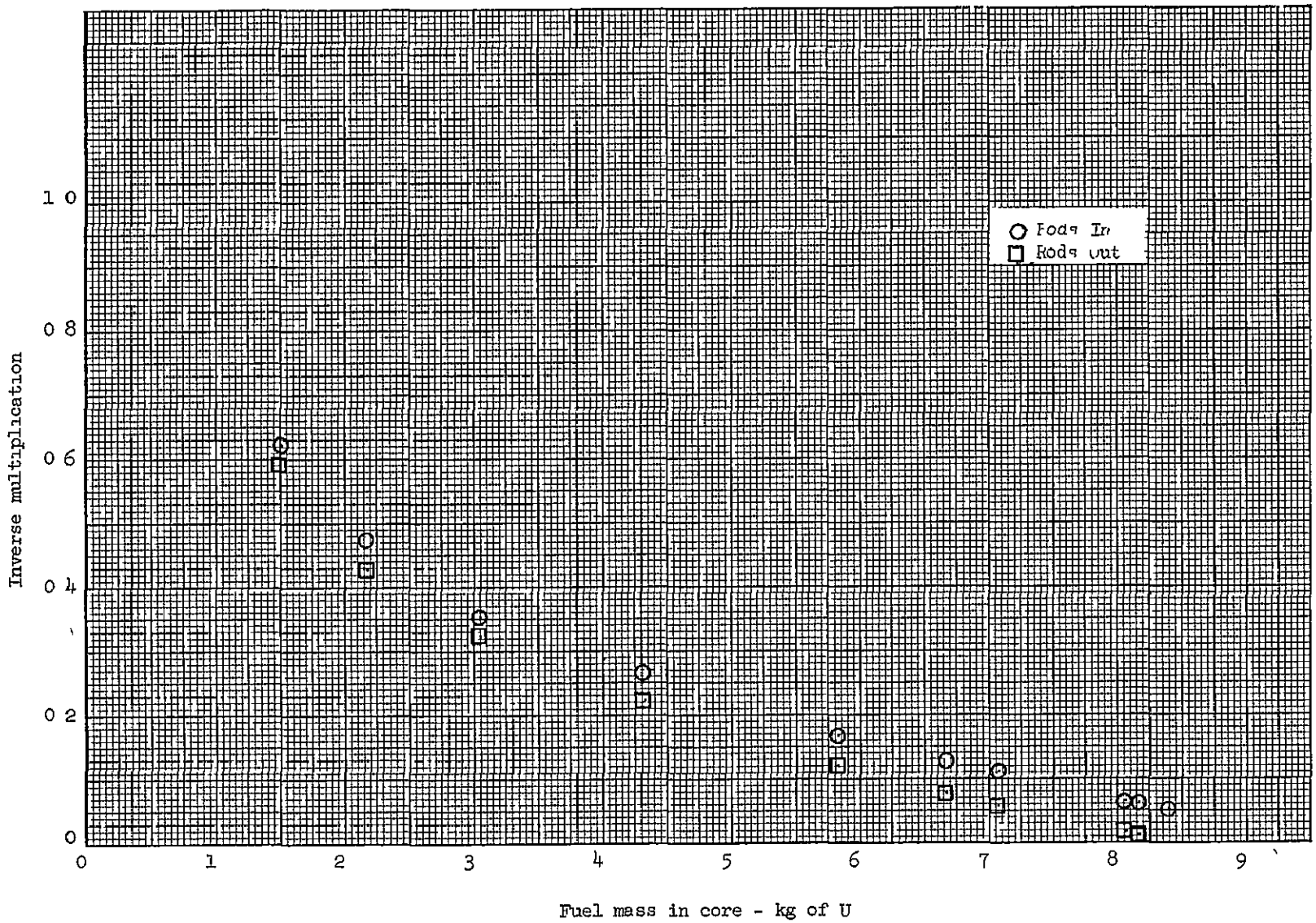


Fig 4.1 Inverse multiplication for initial fuel loading of Configuration #1

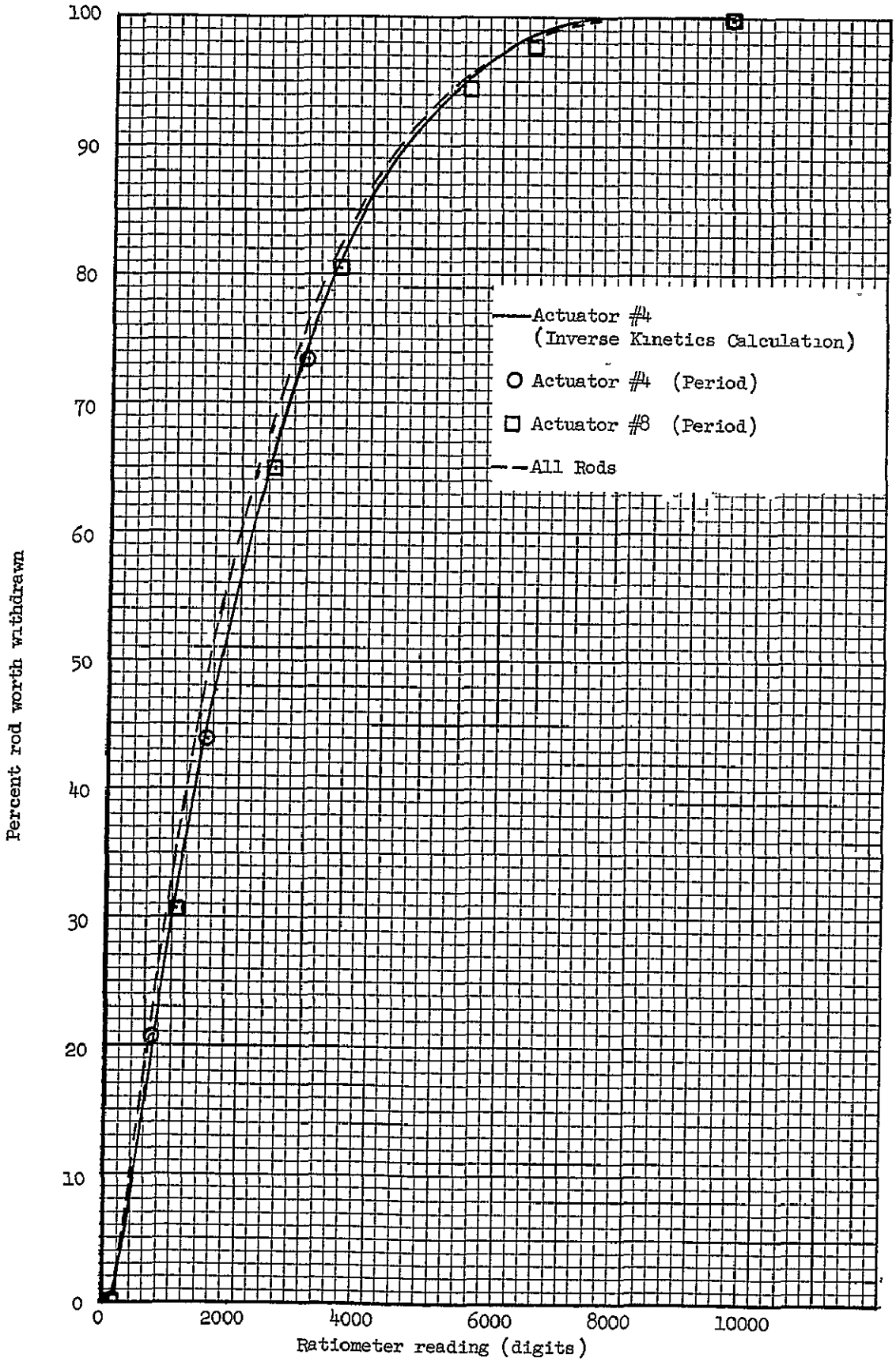


Fig 4 2 Control system rod worth curves

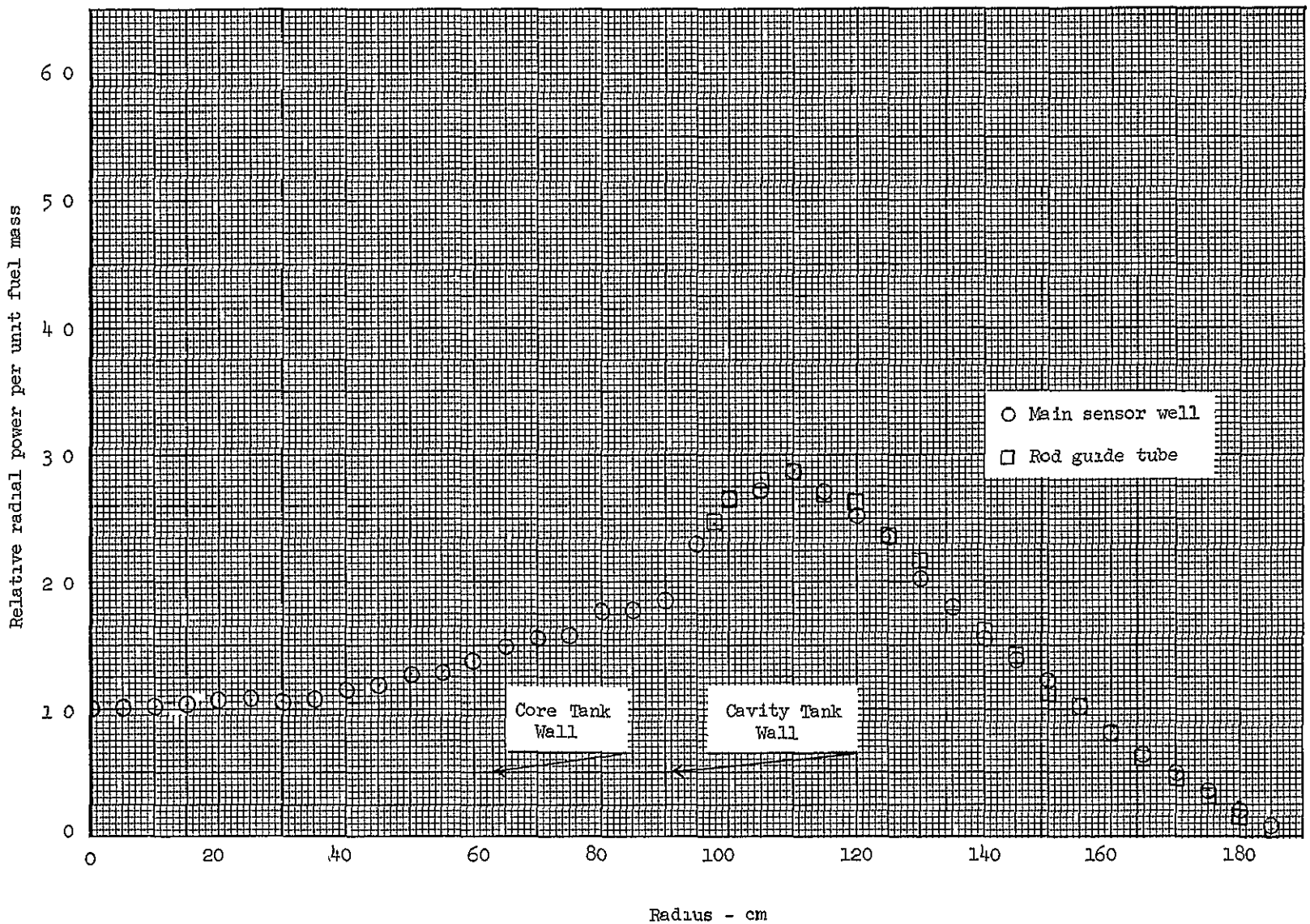


Fig 4 3 Relative specific power (U-235 fission rate) in Configuration #1

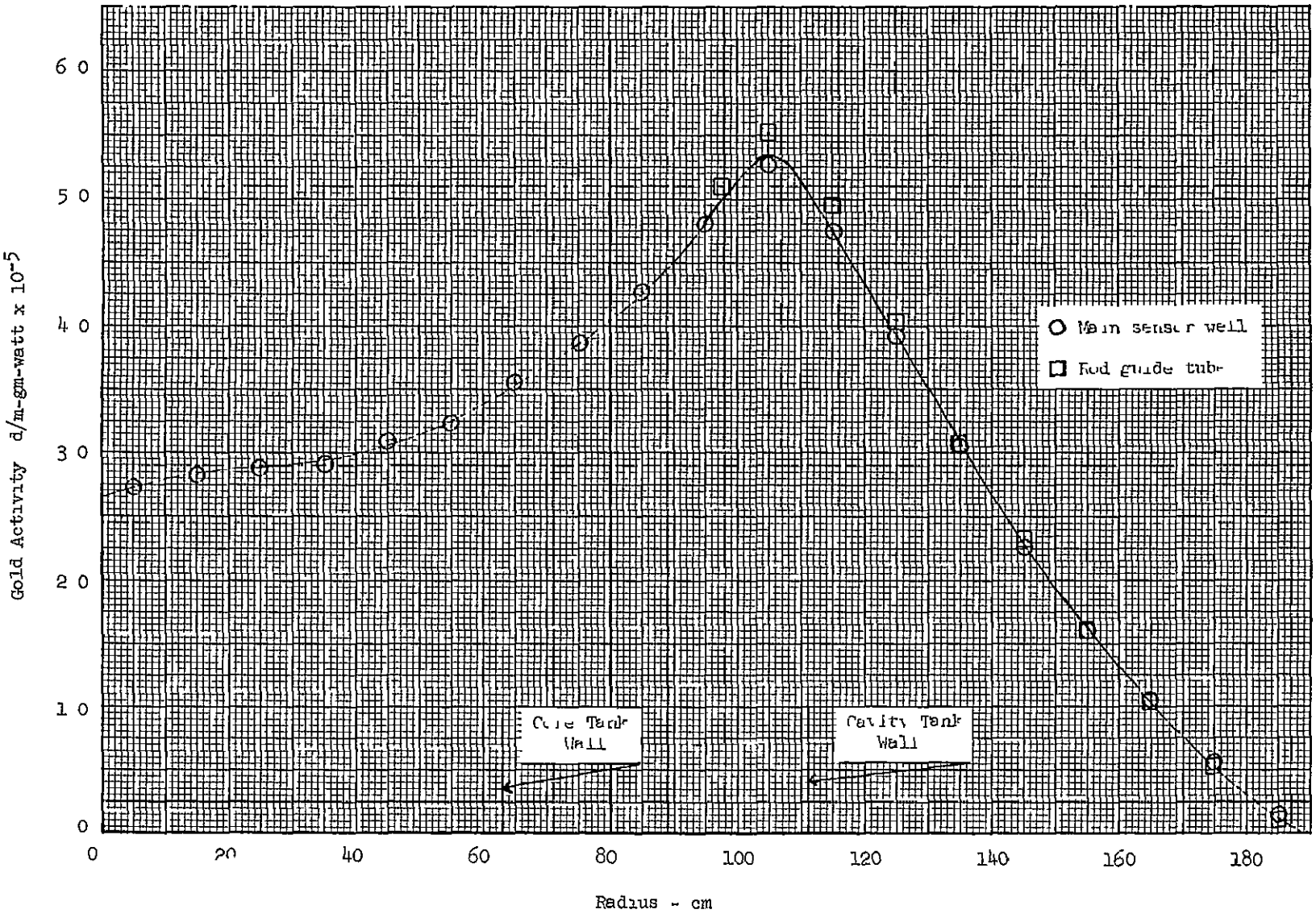


Fig 4 4 Radial bare gold activity (d/m-gm-watt)
Configuration #1

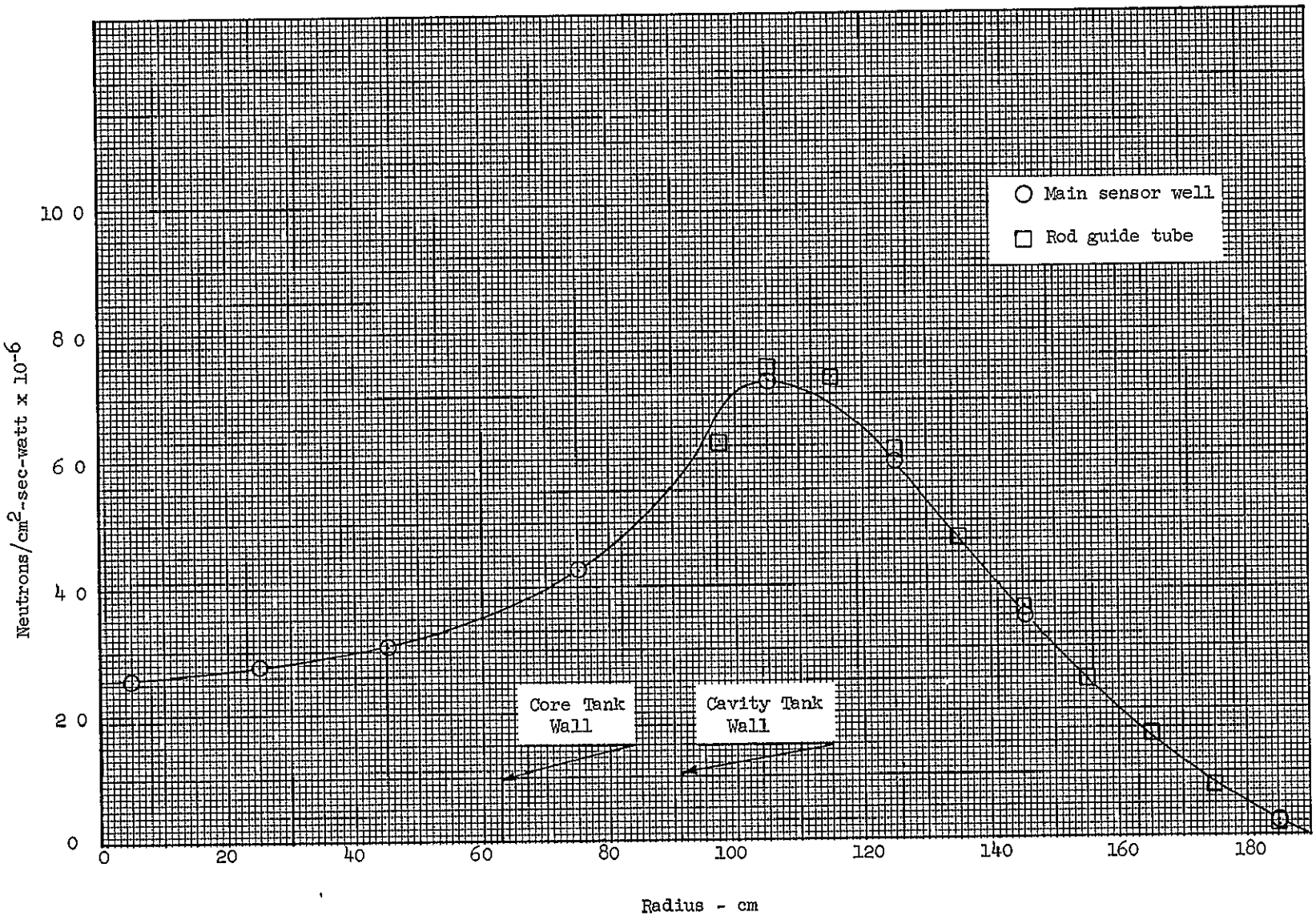


Fig 4 5 Radial gold determined thermal flux
Configuration #1

## 5.0 CONFIGURATION #2 (Hydrogen Propellent Mockup in Cavity Region)

Configuration #2 differed from Configuration #1 in that $1 \times 10^{21}$ atoms/cc hydrogen in the form of foamed polystyrene and polyethelene sheet was installed in the cavity region between the heating air shrouds and the cavity wall. The polyethelene ($CH_2$) was in the form of 0.064 cm thick sheet cut and evenly disbursed throughout the volume while the polystyrene foam (CH) was in the form of both cut sheets (2.54 cm thick) and small cubes nominally 16 4 $cm^3$ for a total mass of 14 23 kg of $CH_2$ and 22 33 kg of CH

The system k-excess before the hydrogen was added to create Configuration #2 was 0.634%Δk/k with 12 880 kg $UF_6$ fuel loading After adding the CH and $CH_2$, $UF_6$ was added to bring the total to 19 505 kg of $UF_6$. A k-excess of 0 454%Δk/k was measured.

## 5.1 Fuel and Coolant Mockup Reactivity Worths

Fuel worth was evaluated by adding a 306 0 gram increment of $UF_6$ to the core raising the k-excess to 0 890%Δk/k, from which a fuel worth of 1.36%Δk/k per kilogram of $UF_6$ or 2.02%Δk/k per kilogram uranium (93.2% $U^{235}$ enriched) was calculated. This compares to 2 96%Δk/k per kilogram uranium for Configuration #1. Assuming a linear worth per kilogram for fuel over the range of fuel loaded (adjusted to $k_{eff} = 1$ for both configuration #1 and #2, 8 46 kg U to 12.91 kg U) the hydrogen mockup propellent was worth -11.0%Δk/k. The assumption of linear worth in this range of fuel densities appears to be justified based on experience with other cavity reactor configurations tested, as shown graphically in Figure 3.3 of reference 3.

The reactivity penalty of the coolant mockup material was somewhat larger than expected from calculations and from the measurement of a lump of $CH_2$ on Configuration #1. This measurement indicated a total reactivity change of 3.57%Δk/k for the mockup while a measurement on the same lump of material in the same position in the reactor (lump positioned in the sensor well between the cavity wall and the core sensor well flange) after installation of the mockup extrapolated to 5 50%Δk/k change, neither of which explained the large 11.0% Δk change determined from the fuel worth measurements and the fuel increment added. A subsequent measurement was made with the lump in the same position but the void above the lump into the $D_2O$ region was plugged with 545 gms of $CH_2$ in an effort to minimize neutron streaming in the sensor well, however the result was nominally the same, i e. a calculated penalty of 5 29%Δk/k for the coolant mockup However, subsequent measurements of the worth of hydrogen made on the stainless configuration (#3) and reported in Section 6 showed a strong effect of spatial dependence and/or effect of flux depression of the core flange on the measurement results This strong spatial dependence has been observed on other configurations (Reference 1, p.251 and 252 and Reference 3, p. 97). In general, these previous experiments showed that hydrogen was worth most when adjacent to the core, least when against the cavity. For this experiment, all of the hydrogen (as CH and $CH_2$) was installed between the outer air-flow shroud and the cavity wall

and thus there was no hydrogen within approximately 5 cm of the $UF_6$ core wall However, the amount of hydrogen installed was equivalent to $1 \times 10^{21}$ H/cc average over the entire region from core to cavity wall

Further difficulties have been encountered with hydrogen in attempts to calculate its worth (See Section 8) and in measured differences in hydrogen worth in CH and $CH_2$ (Ref. 3, p 88). Molecular binding differences between these two molecules could well have a significant effect. The carbon atom contribution to the worth of CH and $CH_2$ is quite small, having been measured previously on a number of other configurations to be between 1 and 8% of the measured worth of the organic molecule (Ref 1, p. 255, Ref. 3, p 88, and Ref. 5, p 38)

## 5.2 Power and Flux Distribution Measurements

Only catcher foils and gold foils were exposed on this configuration The radial power distribution in the sensor well and a rod guide tube is shown in Figure 5.1 Data from the $1\ 2 \times 10^{-3}$ cm thick gold foils are shown as a plot of the bare gold activity in Figure 5.2 and a plot of the thermal flux in Figure 5 3 Catcher foil cadmium ratios (essentially infinitely dilute) are tabulated in Table 5 1 and the infinitely dilute gold cadmium ratios at selected radial positions are given in Table 5.2. All cadmium covered foils were exposed in 0 051 cm(20 mil) thick buckets.

TABLE 5 1

Catcher Foil Cadmium Ratio

Configuration #2

| Radius (cm) | Bare Foil Counts | Cadmium Covered Foil Counts | Cadmium Ratio |
|---|---|---|---|
| Sensor Well | | | |
| 20 | 121029 | 1548 | 78 1 |
| 40 | 140206 | 1557 | 90 0 |
| 60 | 172999 | 1639 | 106 0 |
| 90 | 344540 | 1845 | 187 0 |
| 110 | 488949 | 814 | 601 0 |
| 130 | 362919 | 214 | 1690 0 |
| 150 | 190954 | 434 | 440.0 |
| 170 | 81196 | 237 | 343 0 |
| Guide Tube | | | |
| 105 | 492323 | 5877 | 83 8 |
| 125 | 400736 | 2225 | 180 1 |
| 145 | 233182 | 1241 | 187 9 |
| 165 | 106701 | 300 | 355 5 |
| 185 | 11194 | 42 | 269 1 |

TABLE 5 2

Infinitely Dilute

Gold Foil Cadmium Ratios and Thermal Flux

Configuration #2

| Radius (cm) | Bare Foil d/m/gm-watt x $10^{-5}$ | Bare Foil wt (g) | Cad.Cov.Foil d/m/gm-watt x $10^{-5}$ | Cad.Cov.Foil wt (g) | Infinitely Dilute Cadmium Ratio | Thermal Flux n/cm$^2$-sec/watt x $10^{-6}$ |
|---|---|---|---|---|---|---|
| Sensor Well | | | | | | |
| 20 | 2.065 | .0356 | 1.039 | .0368 | 1.42 | 1.570 |
| 40 | 2.281 | 0348 | 1.020 | .0376 | 1 51 | 1 906 |
| 60 | 2.640 | .0367 | 1.092 | 0351 | 1.63 | 2.432 |
| 90 | 4 240 | .0359 | 1 032 | .0358 | 2.35 | 4 978 |
| 110 | 5.001 | 0359 | 0.387 | .0366 | 6.12 | 7 153 |
| 130 | 3 307 | 0361 | 0.050 | 0359 | 29 40 | 5.053 |
| 150 | 1 878 | .0364 | 0 007 | .0364 | 112.50 | 2 902 |
| 170 | 0 754 | .0370 | 0.002 | 0375 | 163 90 | 1.166 |
| Guide Tube | | | | | | |
| 105 | 5.395 | .0359 | 0.646 | .0348 | 4.23 | 7.379 |
| 125 | 3.908 | .0363 | 0.087 | .0344 | 20 29 | 5.930 |
| 145 | 2.224 | .0354 | 0.007 | 0361 | 131.50 | 3 438 |
| 165 | 0 988 | .0363 | 0.002 | .0369 | 218.90 | 1 530 |
| 185 | 0.108 | 0356 | 0.001 | .0364 | 45.50 | 0.166 |

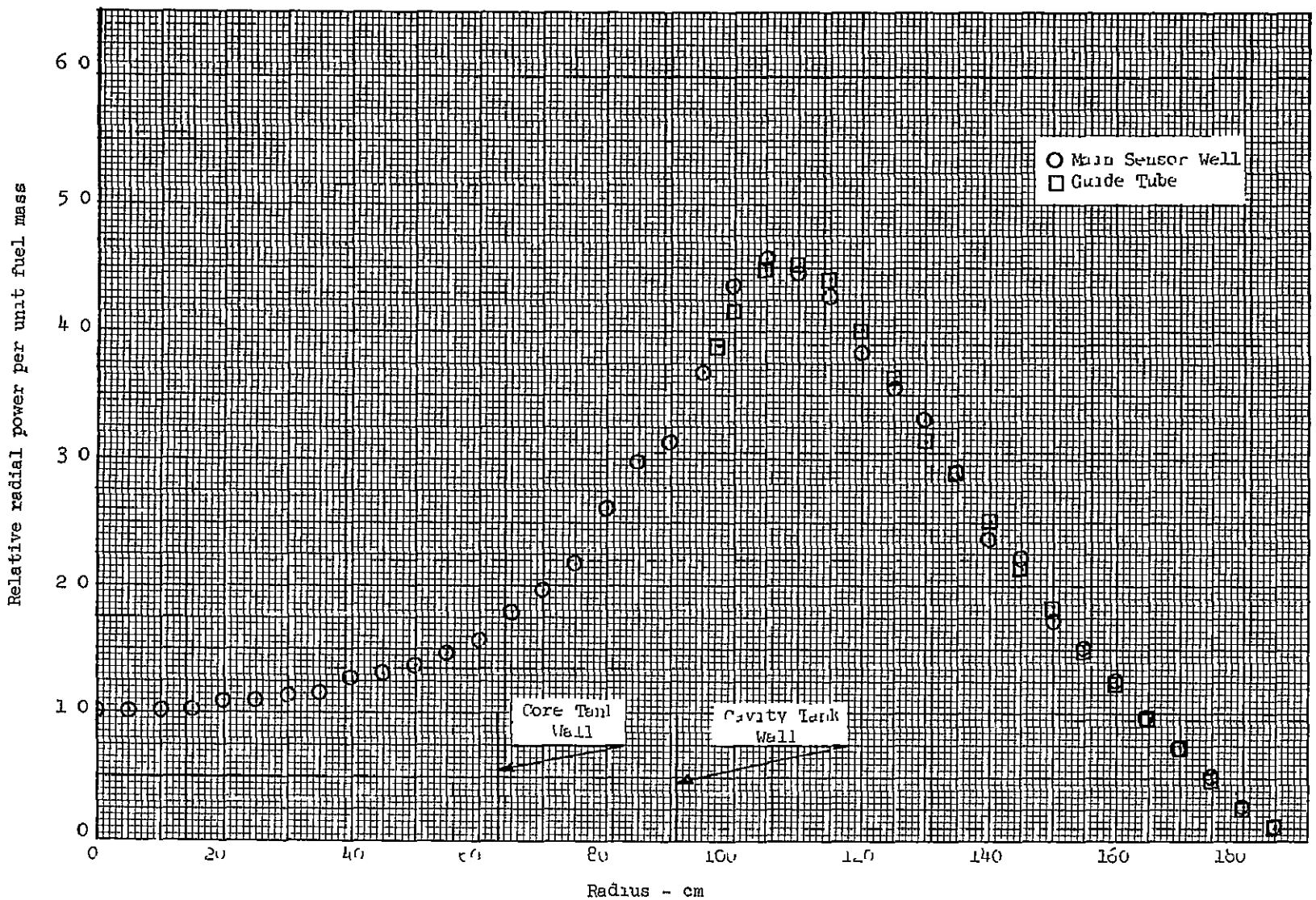


Fig 5 1 Relative Specific Power (U-235 fission rate) Configuration #2

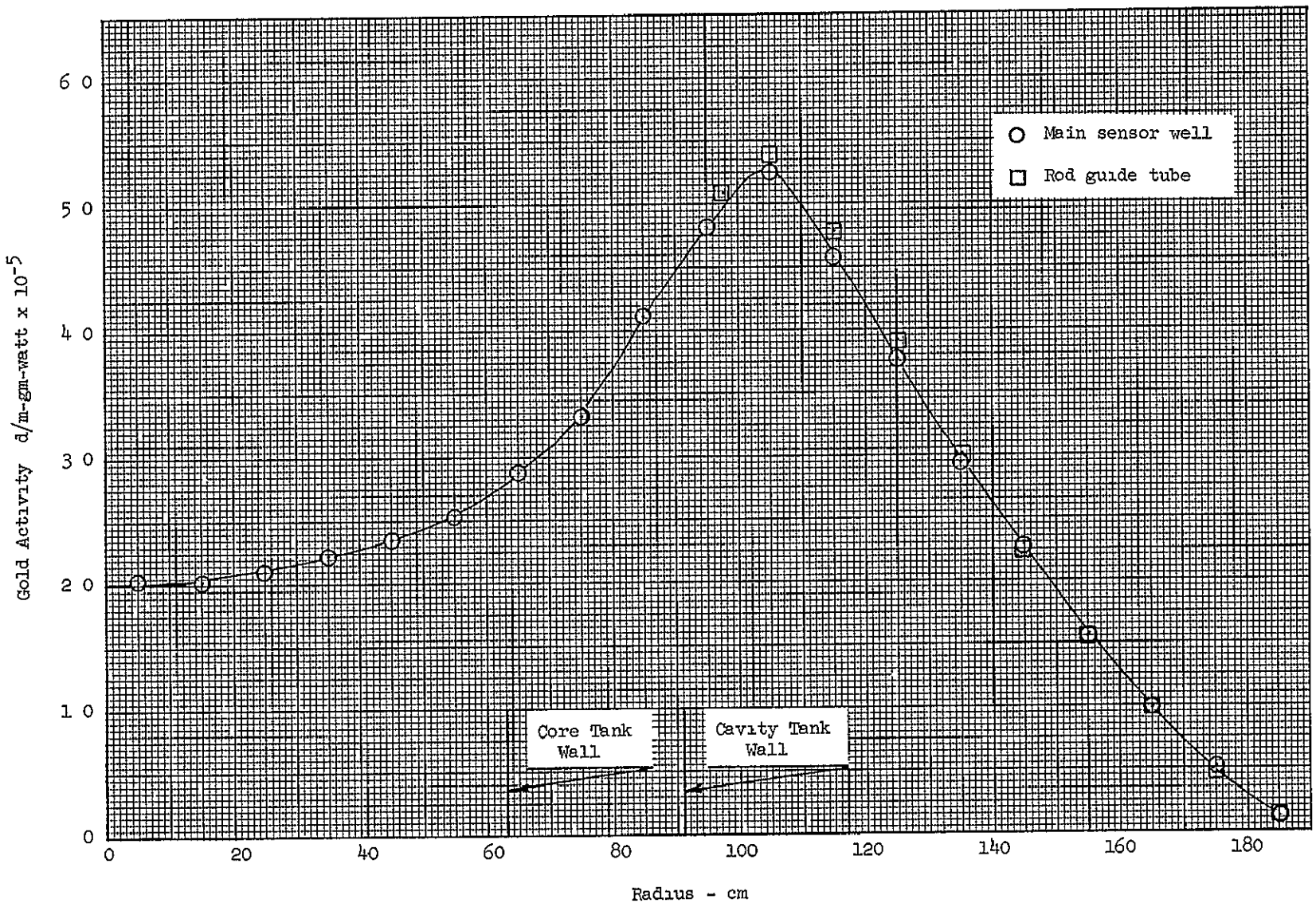


Fig 5 2 Radial bare gold activity (d/m-gm-watt) Configuration #2

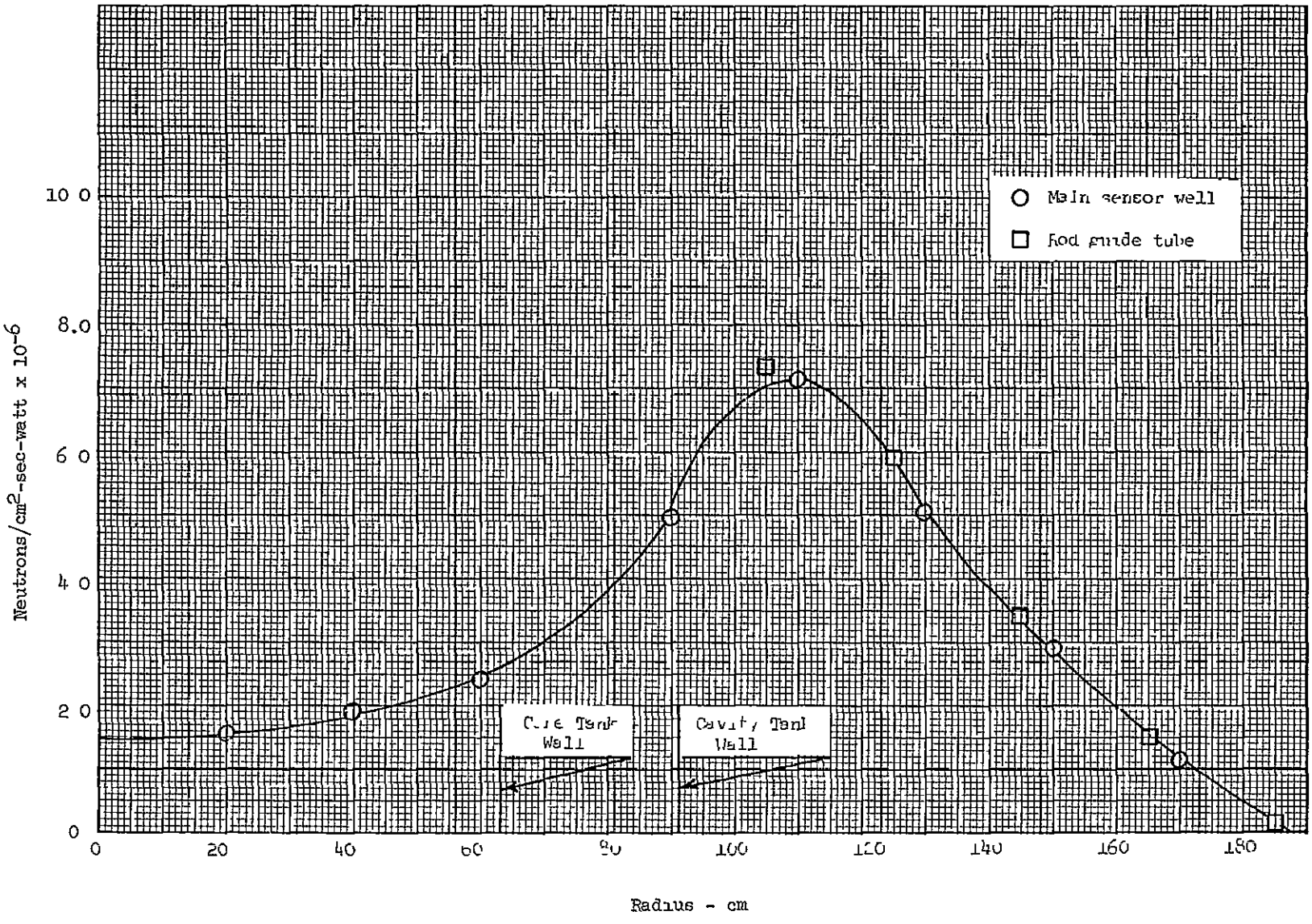


Fig 5 3 Radial gold determined thermal flux - Configuration #2

## 6.0 CONFIGURATION #3 (Stainless Steel Cavity Liner)

Transformation from Configuration #2 (hydrogen) to Configuration #3 (hydrogen plus stainless steel) was accomplished by installing 62.2 kilograms of type 321 stainless steel sheet to the cavity wall to give a nominal SS thickness of 0.0762 cm (30 mils), equivalent to 0.019 mean free absorption paths. The steel, cut to shape from 0.0254 cm thick (10 mil) stock, was installed between the $CH_2$ - CH hydrogen propellent mockup and the outer wall of the cavity

The system k-excess just prior to changing to Configuration #3 was 0.200 %Δk/k with a fuel loading of 19 811 kg $UF_6$ (13 340 kg U) After adding 23 843 kg of $UF_6$ to pay the stainless steel penalty (43.655 kg $UF_6$ or 29 395 kg U total in the reactor) the reactor was critical with 0 0654%Δk/k k-excess The critical loading corrected for fuel in the transfer line and the k-excess is 43.626 kg $UF_6$ or 29 376 kg U

### 6.1 Reactivity and Material Worth Measurements

Fuel worth was evaluated by adding a 429.7 gram increment of $UF_6$ to the core which resulted in a worth of 0 294%Δk/k per kg $UF_6$ or 0 437 %Δk/k per kg U-235 This value compares to 2 02%Δk/k per kg uranium for Configuration #2 with a 13 17 kg U loading and 2 96%Δk/k per kg $UF_6$ for Configuration #1 with a 8 54 kg U loading Using these three fuel worth values, at their respective core loading, and with the aid of Figure 3.3 of Reference 3, a fuel worth vs core loading curve, Fig 6 1, was constructed and the area under the curve between the appropriate limits was integrated to yield a stainless steel worth of -15 3%Δk/k

Direct measurement of stainless steel worth was made by placing narrow strips of 0.091 cm thick (36 mil) stock against the outside of the cavity wall (on the $D_2O$ side). After the stainless steel was installed, a 234 gram sample was measured as a period difference of -0.0285%Δk/k or -0.122%Δk/k per kg which would extrapolate to -7 6%Δk for the entire 62.2 kilogram stainless steel liner A subsequent measurement with a larger 911 gram sample gave a value of -0.161%Δk/k per kg which extrapolates to -10 0%Δk worth for the liner These values can be compared to -0.255%Δk/k per kg measured on Configuration #1 which extrapolates to -15 8%Δk/k for the 67 2 kg liner and is in very good agreement with that value deduced from the fuel worth measurements cited above The steel worth should decrease as the loading becomes heavier, and this was observed. However, the average measured worth is still about 15% less than that deduced from the fuel loading differences. The latter method involved interpolation between three fuel worth points, and conceivably could be in error by this amount

The hydrogen worth between the core and reflector was carefully remeasured The previous results of the reactivity coefficient showed considerable variance (factor of two) from the gross result of the loading change required when $10^{21}$ atoms/cc of hydrogen were added to the cavity (See Section 5 1) A small 3-inch long sample of $CH_2$ weighing

101 gm was measured near the middle of the annular cavity void within the sensor well The sample in this case was three inches from the core top flange and was essentially not influenced by its flux depressing properties The measured worth of polyethylene was -0 60%Δk/kg, 2 to 4 times the previous results (Section 4 2 and 5 1) This latter result, however, extrapolates to a total hydrogen penalty of 15%, compared to the 11% observed between the first two configurations Since the worth varies with fuel loading and other configuration properties, these later results imply consistency, and indicate that the earlier reactivity coefficient results were adversely affected by the presence of the top core flange Note, the carbon worth, less than 10% of the hydrogen worth in $CH_2$, has been ignored

## 6 2 Power and Flux Distribution Measurements

Power and flux distributions over the radius of the reactor were determined in both the sensor well and a rod guide tube by exposing both bare and cadmium covered catcher foils, gold foils, indium foils and manganese foils In addition, cadmium ratios and thermal flux were calculated from the data taken at selected points All cadmium covered foils were enclosed in 0 051 cm (20 mil) thick buckets The method used to calculate the infinitely dilute cadmium ratios and thermal flux are given in Appendix 1

### 6.2 1 Catcher Foil Data

Catcher foil data are plotted as a fine radial power distribution relative to the power at the core center in Figure 6 2 and the cadmium ratio, which is the ratio of the normalized counts from bare and cadmium covered foils exposed at selected radial positions, are given in Table 6 1 Because of the short range of the fission products in the uranium metal foils, these cadmium ratios are essentially infinitely dilute values Therefore they represent the ratio of total to epithermal fission rate

### 6 2 2 Resonance Foil Detector Data - Gold, Indium and Manganese

Figure 6 3 is a plot of radial bare gold activity distribution, of 1 2 x $10^{-3}$ cm thick gold The actual response of foils of this thickness to thermal and epithermal neutrons can be determined by comparing columns 2 and 4 of Table 6 2 However, for general usefulness, the infinitely dilute response of total to epithermal neutrons is preferred, and this is given in column 6 of that table Bare and cadmium covered gold, indium and manganese foils were exposed at selected radial locations in both the sensor well and a rod guide tube The calculated infinitely dilute cadmium ratios and the thermal flux data are shown in Tables 6 2, 6 3, and 6 4 In addition the thermal flux determined from the gold foil activity is plotted in Figure 6 4 All of the data are normalized to a power of one watt as determined from volume weighted catcher foil activity within the spherical core

A final power run at 500 watts and two hour duration was made with special foil packets located at three locations in the sensor well for additional neutron spectrum determination The positions were core center and 61 cm and 105 cm from core center. In each location $^{55}Mn(n,\gamma)^{56}Mn$, $^{127}I(n,\gamma)^{128}I$, $^{63}Cu(n,\gamma)^{64}Cu$, $^{115}In(n,n)^{115m}In$, $^{56}Fe(n,p)^{56}Mn$, $^{64}Zn(n,p)^{64}Cu$, $^{24}Mg(n,p)^{24}Na$, and $^{27}Al(n,\alpha)^{24}Na$ were used.

A multiple foil activation technique (ref 18) employing the SPECTRA (ref 19) code was used to determine the neutron spectrum from the reaction products The thermal flux results (equivalent 2200 m/sec flux) are shown in Fig. 6 4, in which the multiple foil results using Cu, I, and Mn are compared with the standard gold foil results The spectrum at several different locations, from Mev energies to thermal, are shown in Figure 6 5, as relative flux per unit energy Section 8 describes a comparison of these results with the spectrum calculated with a 19-energy group transport code

TABLE 6 1

Catcher Foil Cadmium Ratio

Configuration #3

| Radius (cm) | Bare Foil Counts | Cadmium Covered Foil Counts | Cadmium Ratio |
|---|---|---|---|
| Sensor Well | | | |
| 20 | 56371 | 20802 | 2 710 |
| 40 | 76736 | 22197 | 3 457 |
| 60 | 143159 | 24025 | 5.959 |
| 90 | 403425 | 29319 | 13 760 |
| 110 | 641731 | 12599 | 50 935 |
| 130 | 462736 | 3836 | 120 630 |
| 150 | 251824 | 1455 | 173.075 |
| 170 | 107514 | 659 | 163.147 |
| 185 | 16314 | 244 | 66 861 |
| Guide Tube | | | |
| 110 | 685136 | 12400 | 55 253 |
| 130 | 516206 | 4405 | 117 186 |
| 150 | 229437 | 2240 | 102 424 |
| 170 | 105577 | 1649 | 64 025 |
| 185 | 15493 | 111 | 139 576 |

TABLE 6 2

Infinitely Dilute

Gold Foil Cadmium Ratios and Thermal Flux

Configuration #3

| Radius (cm) | Bare Foil d/m/gm-watt x $10^{-5}$ | Bare Foil wt. (g) | Cad.Cov. Foil d/m/gm-watt x $10^{-4}$ | Cad.Cov. Foil wt. (g) | Cadmium Ratio | Thermal Flux n/cm$^2$-sec/watt x $10^{-6}$ |
|---|---|---|---|---|---|---|
| Sensor Well | | | | | | |
| 5 | 1.066 | .0385 | 8.038 | .0350 | 1 16 | 0.454 |
| 25 | 1 147 | .0308 | 8.274 | .0363 | 1.14 | 0 409 |
| 45 | 1.332 | .0363 | 8.399 | .0367 | 1.25 | 0.758 |
| 75 | 2.538 | .0375 | 9.905 | .0351 | 1.69 | 2 440 |
| 90 | 3.179 | .0356 | 9.509 | .0365 | 2.00 | 3.440 |
| 105 | 4.250 | .0346 | 5.087 | .0363 | 4.16 | 5 790 |
| 125 | 3.131 | .0358 | 0 743 | 0372 | 18.50 | 4 740 |
| 145 | 1.817 | .0368 | 0.090 | .0356 | 84.40 | 2.800 |
| 175 | 0.425 | .0355 | 0.005 | 0351 | 412 00 | 0.659 |
| Guide Tube | | | | | | |
| 97.5 | 4.020 | .0363 | 9.006 | .0363 | 2 49 | 4.840 |
| 115 | 3.971 | .0363 | 2.352 | .0363 | 7.84 | 5.790 |
| 135 | 2.536 | .0364 | 0.215 | 0360 | 51.40 | 3.900 |
| 155 | 1.340 | 0371 | 0.013 | 0362 | 459 00 | 2.080 |
| 175 | 0 421 | .0376 | 0.005 | .0369 | 392 00 | 0 652 |

TABLE 6 3

Infinitely Dilute

Indium Foil Cadmium Ratios and Thermal Flux

Configuration #3

| Radius (cm) | Bare Foil d/m/gm-watt x $10^{-7}$ | Bare Foil wt (g) | Cad. Cov Foil d/m/gm-watt x $10^{-7}$ | Cad. Cov Foil wt. (g) | Cadmium Ratio | Thermal Flux n/cm$^2$-sec/watt x $10^{-6}$ |
|---|---|---|---|---|---|---|
| Sensor Well | | | | | | |
| 5 | 3.204 | .00584 | 2.368 | .00649 | 1 22 | 0 638 |
| 35 | 3.665 | 00518 | 1.061 | 00516 | 2.75 | 2 160 |
| 60 | 4 746 | .00512 | 2.635 | .00515 | 1.56 | 1.730 |
| 90 | 7.738 | .00740 | 2.651 | .00515 | 2.43 | 4.430 |
| 105 | 9.060 | .00584 | 1.426 | .00740 | 4.41 | 6 260 |
| 120 | 7.596 | .00518 | 0.424 | .00518 | 13.00 | 5 960 |
| 145 | 3.923 | 00512 | 0.137 | 00679 | 19.20 | 3.140 |
| 170 | 1.166 | .00740 | 0.003 | 00519 | 248 00 | 0 966 |
| 185 | 0.239 | .00510 | 0.0006 | .00679 | 283.00 | 0.198 |
| Guide Tube | | | | | | |
| 135 | 2.399 | .00510 | 0.007 | 00562 | 52 60 | 4 420 |
| 155 | 2.483 | 00649 | 0.0007 | .00516 | 261 00 | 2.060 |

TABLE 6 4

Infinitely Dilute

Manganese Foil Cadmium Ratios and Thermal Flux

Configuration #3

| Radius (cm) | Bare Foil d/m/gm-watt x $10^{-5}$ | Bare Foil wt (g) | Cad.Cov.Foil d/m/gm-watt x $10^{-4}$ | Cad.Cov.Foil wt | Cadmium Ratio | Thermal Flux n/cm$^2$-sec/watt x $10^{-6}$ |
|---|---|---|---|---|---|---|
| Sensor Well | | | | | | |
| 5 | 4.368 | .0433 | 12 720 | .0460 | 2.15 | 0.692 |
| 35 | 5.648 | .0437 | 13.180 | 0420 | 2.62 | 0.980 |
| 60 | 5.262 | .0432 | 13.410 | .0410 | 2.46 | 0 889 |
| 90 | 28.770 | 0415 | 13.580 | .0460 | 10.60 | 6 160 |
| 105 | 44.950 | .0427 | 33.760 | 0433 | 6.96 | 9.360 |
| 120 | 39.580 | .0426 | 1.845 | 0480 | 101.00 | 8.870 |
| 145 | 21.920 | .0415 | 0.116 | 0440 | 909 00 | 4.930 |
| 170 | 7 613 | .0430 | 0.049 | .0438 | 743 00 | 1 710 |
| 175 | 4.972 | .0430 | 0.020 | .0423 | 1237 00 | 1 120 |
| 185 | 1.168 | .0459 | 0.037 | 0430 | 152.00 | 0.212 |
| Guide Tube | | | | | | |
| 97.5 | 9.740 | .0424 | 12.420 | .0468 | 8 00 | 4 160 |
| 120 | 41.920 | .0480 | 0.826 | .0438 | 245 00 | 9 420 |
| 135 | 1.465 | .0434 | 0.326 | .0423 | 22.40 | 0.323 |
| 155 | 15.950 | .0456 | 0.035 | .0467 | 2160 00 | 3.590 |
| 170 | 3.540 | .0439 | 0.051 | 0459 | 328 00 | 0.796 |

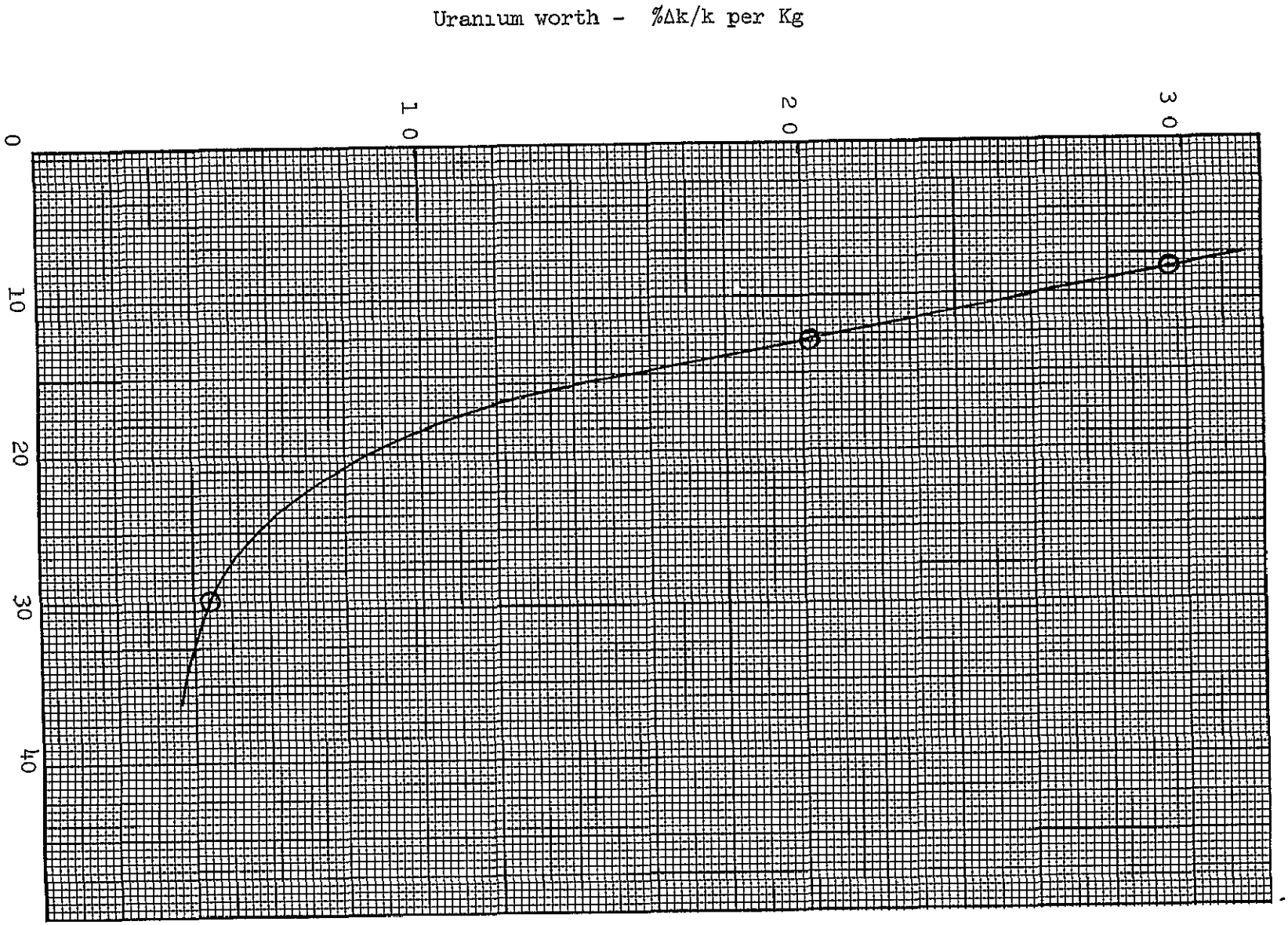


Fig 6 1 Fuel Worth vs Core Loading

Fig 6 2 Relative specific power (U-235 fission rate) Configuration #3

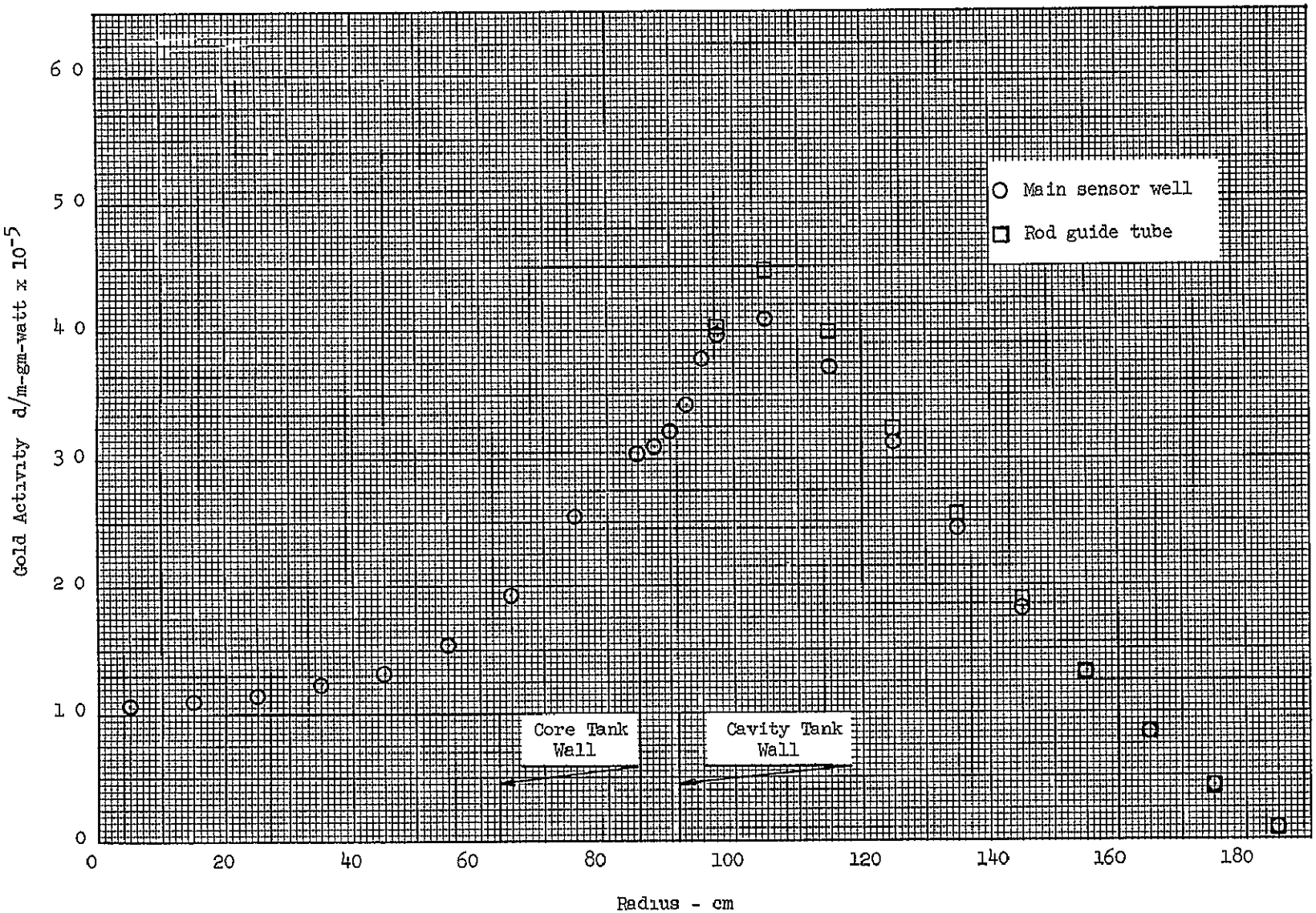


Fig 6 3 Radial bare gold activity (d/m/gm-watt) Configuration #3

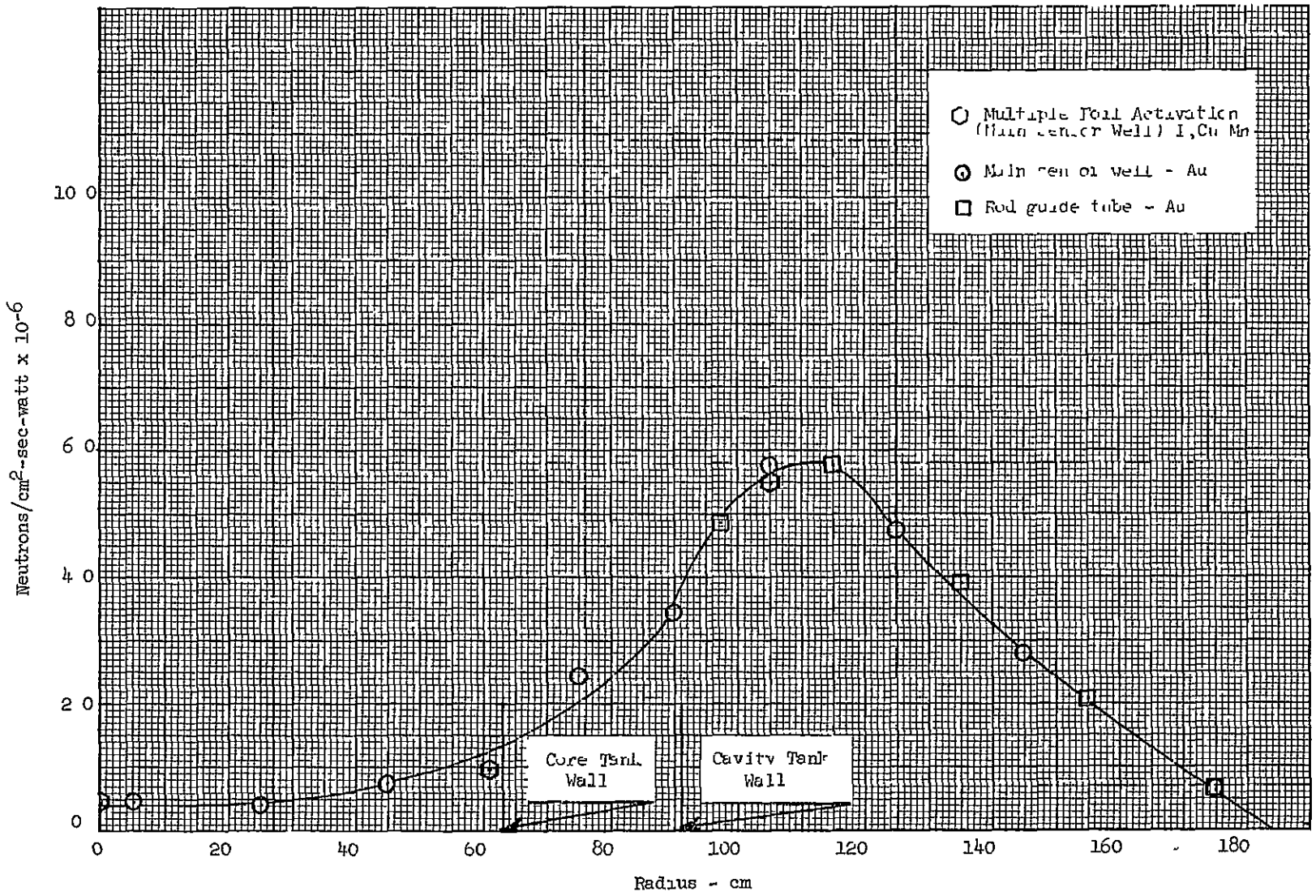


Fig 6 4 Radial gold determined thermal flux - Configuration #3

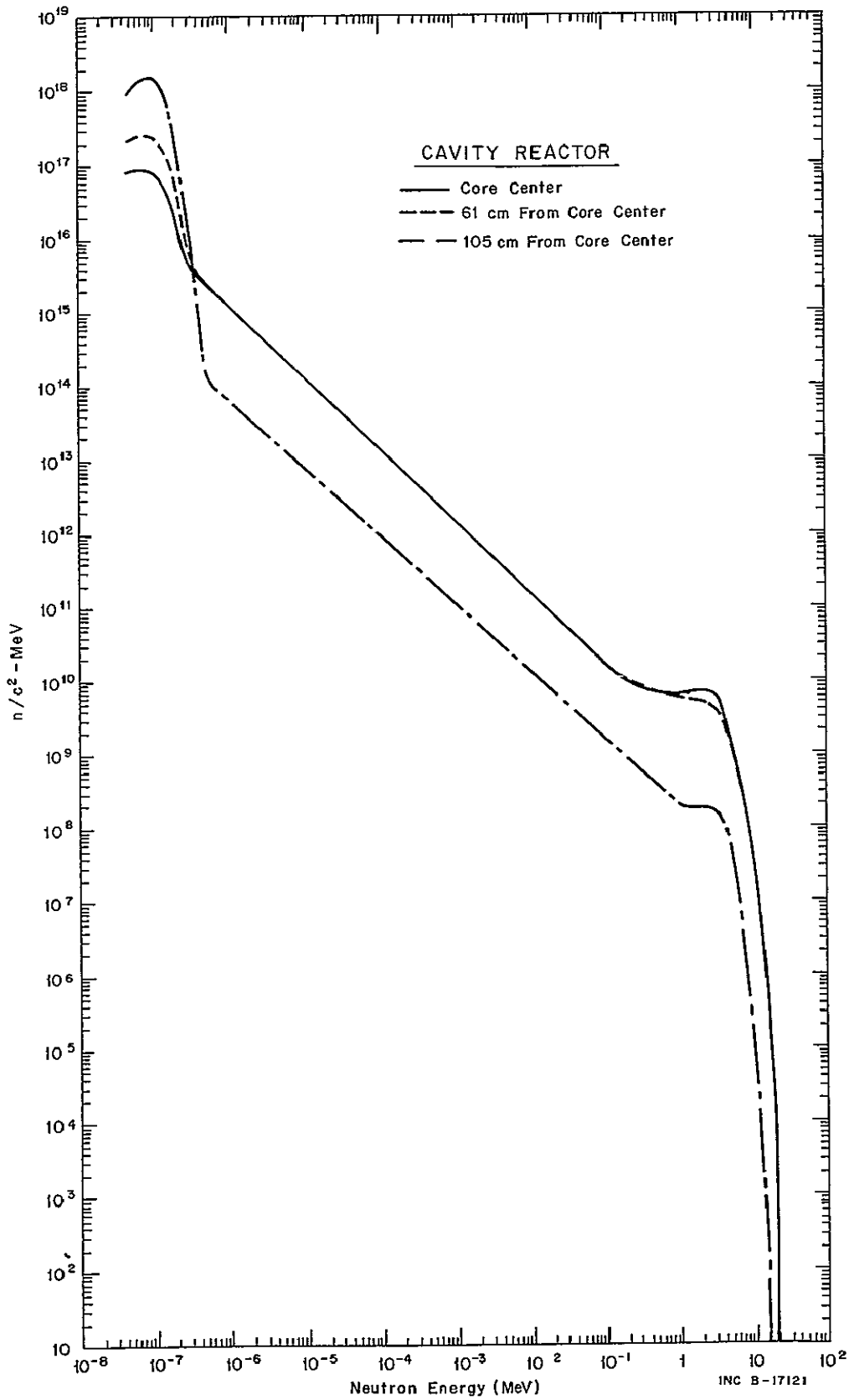


Fig 6 5 Neutron spectrum determined from multiple foils activation

## 7.0 CONTROL SYSTEMS EVALUATIONS

The gas core will require substantial reactivity control to compensate for fluctuations in the reactivity created by shifts in the boundary between the hydrogen and uranium. Waves of the order of 2% to 3%$\Delta k$ might occur (Ref. 4). Therefore, an experimental study of a number of control systems was performed on Configuration #3.

### 7.1 Designs

The heavy water ($D_2O$) reflector of the gas core (cavity) reactor offers an ideal location for control devices. The commercial grade of $D_2O$ has a mean free absorption path length for thermal neutrons of about 12,000 cm Thus poison, even if placed only as discrete chunks in the reflector will substantially increase the absorption Also, the average thermal flux in the reflector is 3 to 4 times what it is in the core, making absorption cross section added to the reflector particularly effective as a control method.

Several methods of moving poison control devices within the reflector can be envisioned. Four such devices measured with this reactor are shown schematically in Figure 7 1 The control rod method was utilized as the principal control device for operation of the critical The control drum method has been used in some other reactor designs having cylindrical reactor boundaries. Control drums appear somewhat awkward when inserted in a spherical reflector, but nevertheless short drums can be fit into the system The cap ("skull cap") and sleeve are schemes generally peculiar just to this type of reactor They can very conveniently be designed into a spherical reflector. The dimensions of these control devices are shown in the sketches (Figure 7 1). Cadmium was the absorber material for all except the control rods, which contained boron carbide

### 7 2 Measurement Method

Since all of the control devices considered must provide large amounts of reactivity control, evaluation of their worth requires techniques that can measure values of 2 to 20 dollars of reactivity Operationally (and perhaps analytically) the prompt neutron decay via the pulsed neutron method is the most direct evaluation technique Reference [12], for instance, is a relatively thorough article reviewing some of the now standard techniques, and it discusses their limitations and uncertainties. The reader is referred to this article and the subsequent article in the same issue for general background information

In the case of the gas core cavity reactor, only the so-called Simmons-King (ref. 13) method of direct evaluation of reactivity from the decay rate of the pulse is generally applicable The area-ratio methods of Sjöstrand, Gozani, and Garelis and Russell can only be used for evaluating highly subcritical conditions of 5 dollars or more This is because at lower levels of subcriticality the prompt neutron decay rate is of the same order of magnitude as that of the fastest delayed neutron group

(1/3 second mean lifetime or $\lambda = 3\ sec^{-1}$) Hence, only for total control system worth was an area-ratio method attempted However, the time-budget limitations on the experiment generally left much to be desired in the accuracy and usefulness of this data

The system was pulsed through a thimble-type tube extending into the reflector. The neutron producing target was approximately 2 cm from the cavity wall The neutron decay was monitored with a small boron coated chamber inserted into an empty control rod guide tube until it nearly touched the cavity wall. Pulse widths were approximately one millisecond or less, repetition rates between 0 5 and 3 pulses per second, depending on the speed of the decay Thus, even for the fastest repetition rate used the delayed neutron background was not constant (though the small correction for the fastest delayed groups could be made with little overall uncertainty fro the 3 pulse/second rate) All decay data was monitored with a 256 channel time analyzer A typical plot is shown in Figure 7 2. The pulse "buildup" extends for a modal contamination, which is not unexpected unless the detector and source could both be placed near the reactor center

## 7 3 Results of Pulsed Neutron Data

Because of the overlap of the faster delayed neutron decay rates with that of the prompt decay, the Simmons-King (ref 13) (or $\alpha$-method) was the principal method used for converting $\alpha$ to reactivity All of the data was analyzed by least squares fitting to a single exponential plus background, $\phi = Ae^{-\alpha t} + B$, three parameters. Double exponential fits yielded nothing significant other than a long decay component approximately equal to the average delayed neutron decay constant The results of the various measurements are shown in Table 7 1 To apply the Simmons-King $\alpha$-method, one must know the prompt neutron lifetime. Unfortunately, the lifetime varies with the amount of control inserted into the reactor The 1/v-lifetime was calculated, using a 19-group diffusion code, to be 2.4 milliseconds without control in the reflector With all the control rods inserted (3.5% subcritical), the calculated lifetime was 2 14 milliseconds However, the measurements at or near critical vs those with the control rods inserted showed the reverse (and unexplainable) trend, 2 52 milliseconds near critical but 2 9 milliseconds with control rods in A thorough experimental investigation of this anomaly was precluded by programmatic obligations It is assumed that the location of the chamber, surrounded by control rods, involved long-lived higher order harmonics These then influenced the apparent decay, giving a different result from the fundamental mode, uniformly poisoned reflector, which the calculation simulated for the control system worth

The results for the worths of the four main control systems measured were deduced from the calculated and measured lifetimes, and appropriately averaged

| | Total Worth %Δk/k | Worth $\frac{\%\Delta k/k}{cm^2}$ |
|---|---|---|
| 23 Control Rods* | (3 8 ± 0 4) | |
| 1 Control Drum | (2 0 ± 0 3) | $1\ 44 \times 10^{-3}$ |
| 1 Cap | (3 9 ± 0 5) | $1\ 58 \times 10^{-3}$ |
| 1 Sleeve | (17 ± 4 0) | $96 \times 10^{-3}$ |

(Note One dollar = 0 788%Δk)

Figure 7 3 shows the worth shape curves of these four control methods

All of these control methods provide large control margins, if one considers using a number of drums or caps (such as six) The worths of six will not be six times the worth of one But the effect of interactions of the control elements is not sufficient to alter the conclusion that large amounts (order of 10%Δk and above) can be achieved by reflector control schemes, despite the uncertainties in the experimental results

---

*This value is that from the inverse kinetics analysis, and is about 12% lower than the incremental summed rod worths It does, however, give the best consistency with the overall pulsed neutron results

TABLE 7.1

Decay Constants for Control Systems

| Configuration Measured | α in 1/milliseconds |
|---|---|
| Control Rods | |
| 0.55% subcritical* | 0 0054 ± 0 0006 |
| 3.54% subcritical* | 0 0149 ± 0.0002 |
| Single Drum | |
| Position of Poison | |
| 0° (toward core) | 0.01095 ± 0.00004 |
| 45° | 0.0062 ± 0.0001 |
| 90° | 0 0043 ± 0.0001 |
| 135° | 0 0032 ± 0.0001 |
| 180° (pointing outward) | 0.0034 ± 0 0003 |
| Cap | |
| Cm from Cavity Wall | |
| 2.5 | 0.0163 ± 0 0001 |
| 12.5 | 0.0125 ± 0.0002 |
| 30.5 | 0.0075 ± 0 0002 |
| 61 | 0 0046 ± 0.0003 |
| Sleeve | |
| Cm that Center is above Midplane | |
| 18 | 0 077 ± 0.001 |
| 30 | 0.077 ± 0.001 |
| 45 | 0 0575 ± 0.0004 |
| 76 | 0 0289 ± 0 0004 |

*Known from previous control rod calibrations using inverse kinetics and bump period

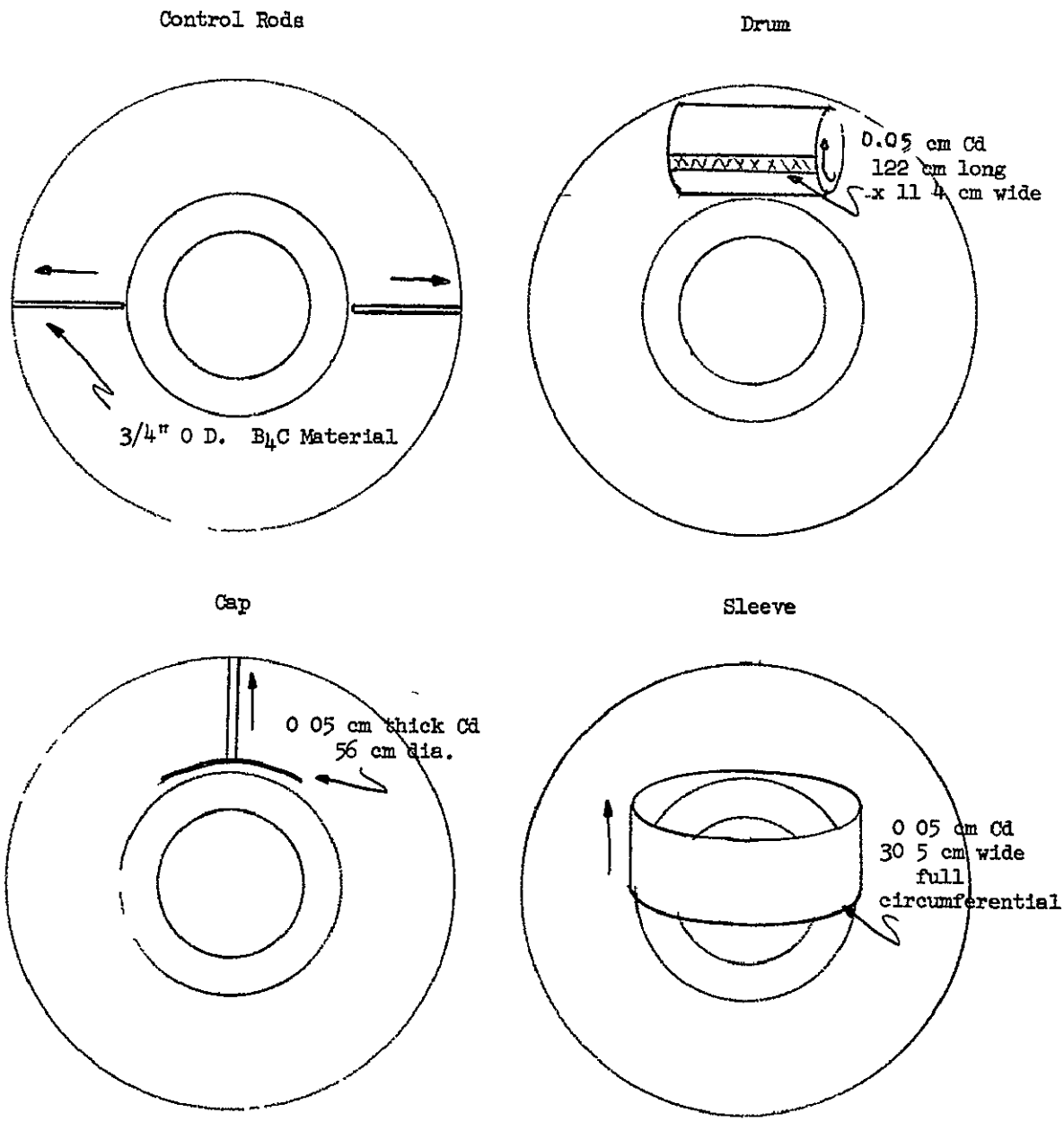


Figure 7 1 Control Schemes

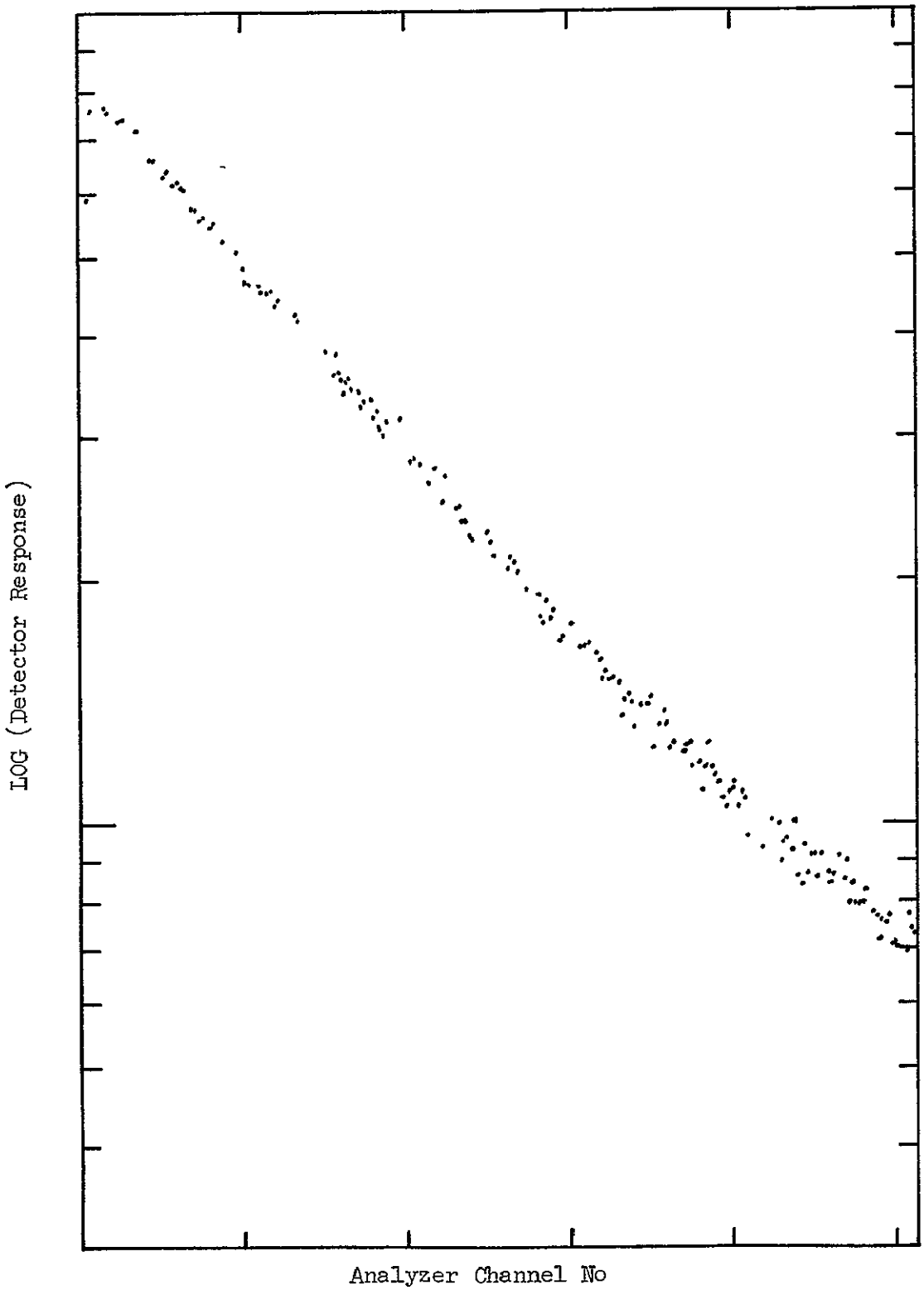


Figure 7 2 Typical Detector Response Plot
(All Control Rods In)

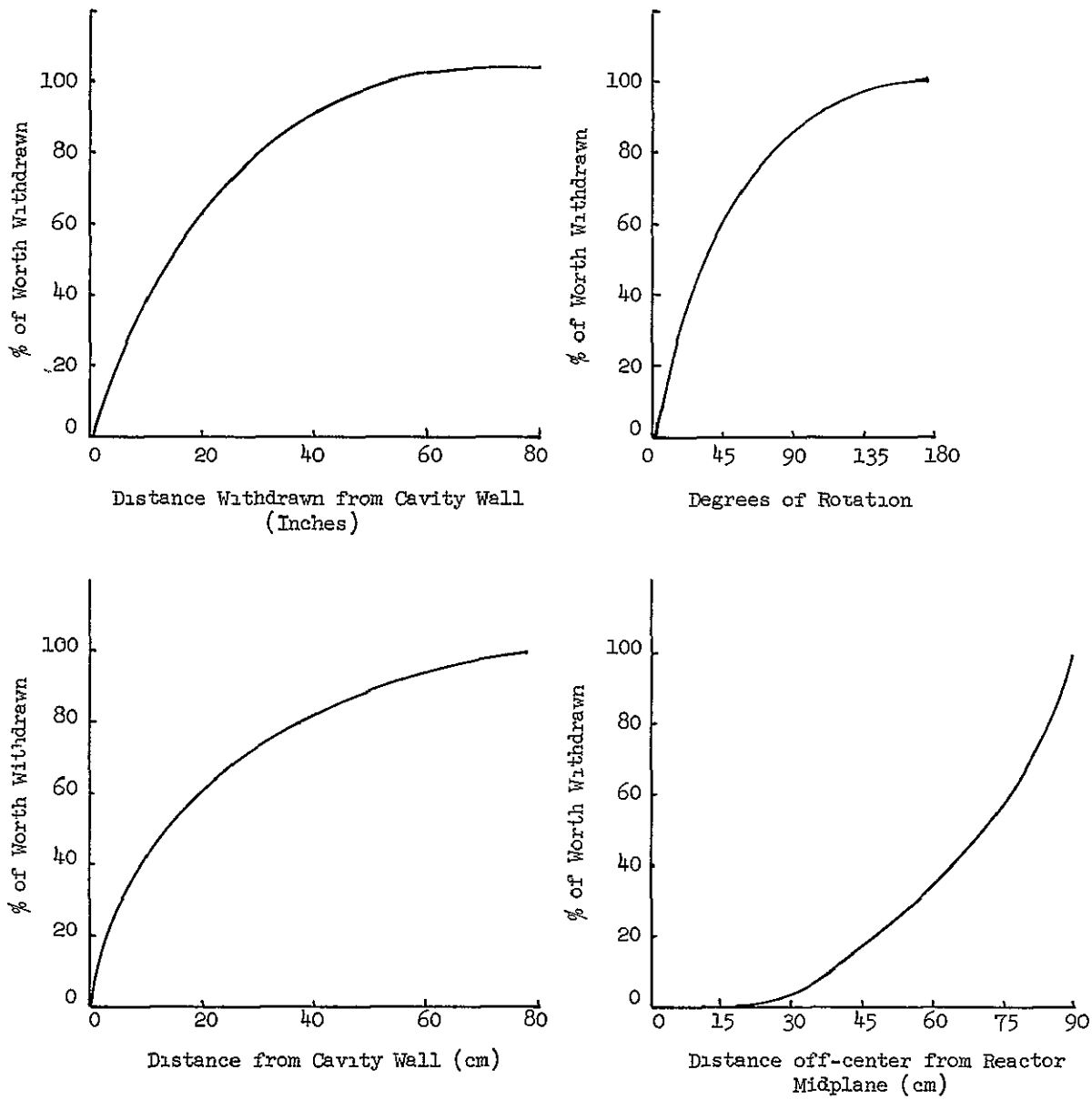


Figure 7.3 Control Worth Shape Curves

## 8 0 ANALYTICAL CALCULATIONS

Reactor physics calculations were performed on the three basic configurations using multi-energy-group computer codes Because of the spherical symmetry of the configuration, all calculations were carried out in one-dimensional spherical geometry A diffusion theory code using 19 energy groups with only one Maxwell-Boltzmann thermal group was used for routine operational predictions For calculating absolute values of k-effective this code gives a bias factor of about 3% However, for predicting k-excess differences for minor changes in a configuration, the code is a useful reactor operational tool

The principal calculations to predict the initial fuel loadings for each configuration were performed with a $S_n$-transport theory code, SCAMP (ref 14) The analyses were all done in $S_4$ angular detail Reference 6 discusses the sensitivity of gas-core reactor calculations to the space energy and angle parameters The spatial detail with one dimensional calculations could use a much finer mesh than was used in the two dimensional calculations reported in Reference 6 In this spherical geometry, 62 mesh points were usually employed For energy group structure, 12 fast and slowing down groups and 7 thermal groups with up scatter were employed, for a total of 19 energy groups The energy group structure is given in Table 8 1 The fast cross section were obtained from a 99-group GAM-II tape modified for use with the PHROG (ref 15) (Phillips-Hanford Revision Of GAM) code The thermal cross sections were obtained from the code INCIT$_E$ (ref 16), similar to GATHER The cross sections obtained from the Idaho codes were compared to those obtained from GAM-GATHER codes at the Lewis Research Center, and appropriate corrections were made to obtain the ostensibly most satisfactory set possible from the two sets of codes

With the detail specified above in angle, space, and energy, typically 120 to 150 outer iterations had to be run before k-effective was converged to within 0 0001 and the pointwise fluxes to within 0 0002 The initial calculations were done with the support column aluminum and void homogenized throughout the $D_2O$ reflector The predicted critical mass for the first configuration was 8 4 kg The actual measured mass turned out to be 8 434 kg after applying the various corrections for the support column Strangely, the calculated fuel worth was low by 50% compared to the measured value of 2 96%$\Delta k$/kg U Despite the good success on the critical loading prediction, success was not as good on the other two basic configurations Initial calculations on these, grossly underpredicted the critical loading Calculated k-effectives were high by as much as 10% One cause of this serious discrepancy was an incorrect scattering kernel for polyethylene in the low energy thermal groups When the water kernel was used for hydrogen, the bias on k-effective was reduced to about 3%$\Delta k$ for these last two configurations Most of this bias is attributed to the hydrogen in the form of CH and $CH_2$ The absorption cross sections are probably correct, but the scattering is suspected as being the major calculational problem The <u>change</u> from Configuration 2 to Configuration 3, which was the addition of 0 075 cm of stainless steel to the cavity was calculated to within 0 5%$\Delta k$ The total worth of the change was experimentally determined to be -15 3%$\Delta k/k$ Table 8 2 is a summary of the calculated eigenvalues for the three configurations measured in this experiment

There appear to be no other major problems with the analytical calculations except that with hydrogen worth and fuel worth The calculated spectra were equivalent to the measured spectra, within the accuracy of the measurements (See Section 9 0) The inability to accurately predict fuel worth has been a general problem in previous work (ref 6) and the reason for the discrepancy is not understood This problem does lead to some concern for the ability to predict criticality accurately with other fuels (Pu-239or U-233) However, the hydrogen discrepancy is far too severe, and deserves more immediate attention The sensitivity of the calculation to the hydrogen scattering kernels needs to be evaluated, and then the correct kernels for the hydrogen in the experiment must be developed Ironically, the operation of a gas core at high temperatures involves major changes in the hydrogen scattering properties and the absorption of uranium fuel Since neither of these materials are ostensibly being handled correctly at present at "room" temperatures, the high temperature calculations are considerably in doubt Some of the high temperature hydrogen effects are covered in Reference 17

TABLE 8 1

Cross Sections 19-Energy Group Format

| Group | Lower Lethargy | Lower Energy (Mev) |
|---|---|---|
| 1 | 1.0 | $3\ 7 \times 10^{0}$ |
| 2 | 1 5 | $2\ 2 \times 10^{0}$ |
| 3 | 2 0 | $1\ 4 \times 10^{0}$ |
| 4 | 3 0 | $5\ 0 \times 10^{-1}$ |
| 5 | 4 0 | $1\ 8 \times 10^{-1}$ |
| 6 | 5 0 | $6\ 7 \times 10^{-2}$ |
| 7 | 6 0 | $2\ 5 \times 10^{-2}$ |
| 8 | 8 0 | $3\ 4 \times 10^{-3}$ |
| 9 | 10 0 | $4\ 5 \times 10^{-4}$ |
| 10 | 12 0 | $6\ 1 \times 10^{-5}$ |
| 11 | 14 0 | $8\ 3 \times 10^{-6}$ |
| 12 | 15 25 | $2\ 4 \times 10^{-6}$ |
| 13 | 17 0 | $4\ 1 \times 10^{-7}$ |
| 14 | 17 7 | $2\ 0 \times 10^{-7}$ |
| 15 | 18 24 | $1.2 \times 10^{-7}$ |
| 16 | 18 65 | $8.0 \times 10^{-8}$ |
| 17 | 19 80 | $2\ 5 \times 10^{-8}$ |
| 18 | 21 41 | $5\ 0 \times 10^{-9}$ |
| 19 | -- | 0 0 |

TABLE 8 2

Calculated Eigenvalues for Three Configurations

| Nuclear Model of Table 4 1 | Fuel (kg U) | Calculated k |
|---|---|---|
| Configuration #1 | 10 0 | 1 058* |
| Configuration #2 | 13 3 | 1 180 |
| Configuration #3 | 29 2 | 1 175 |

*The 10 kg U loading was the smallest loading calculated A correction was made, using a fuel worth value based on measurements in previous cylindrical geometry experiments (Ref 3) of 0 32%Δk/kg U, which yield the predicted critical mass of 8 4 kg U This prediction allows for the 0 70%Δk net penalty of the support columns and fuel line, which are non-spherical perturbations (see p 14)

## 9 0 DISCUSSION OF EXPERIMENT AND RESULTS

This experiment represents the second all gas core reactor critical experiment It is the first simple, clean, spherical geometry experiment of its type and hence should be quite useful as a benchmark experiment The first all-gas-core experiment was operated in 1967 (ref 2) without incident. In the spherical experiment just completed, one minor leak incident occurred when a $UF_6$ valve diaphragm ruptured during a heat-up operation A few grams (less than 10) of $UF_6$ were lost from the system, insufficient to noticeably alter the apparent critical mass results Otherwise, the operation of the experiment was without incident

The approach to criticality as the reactor was heated and the converse cooldown provided some interesting effects Selective evaporation and cooldown were observed, as shown in Fig 9 1. In this figure, the indicated "average" core temperatures are merely the average of four thermocouples placed at the top, middle and bottom of the outside wall and at the center (through the flux monitor tube) As the core is being heated from a shutdown condition, the fuel is most likely being evaporated from a large solid and/or liquid pool at the bottom of the sphere (depending on the pressure) As the core cools, selective condensation occurs on the cool spots of the wall first, then on the entire wall as the wall temperature equalizes. As the layer on the wall thickens, it eventually drops off or runs off to the bottom of the sphere There is probably an optimum thin thickness of condensed fuel on the wall that gives a peak in reactivity, but a very large spike was not observed in this experiment as had been observed in the first $UF_6$ gas core experiment (ref 2)

The ostensible temperature-reactivity coefficient shown in Figure 9 1 is caused by evaporation or condensation of the last or initial, respectively, amounts of fuel, and is therefore not a true temperature coefficient, such as due to sphere expansion This latter coefficient was, for all practical purposes quite small and essentially unmeasurable (less than 0 001%$\Delta k/°C$)

Multiple foil packets for obtaining neutron spectral data were exposed for two hours during a reactor run at 500 watts power During this run it was possible to maintain the $UF_6$ gas core at a sufficient temperature from nuclear heating to keep the core above the $UF_6$ vaporization temperature and the external electrical heat source normally used could be shut down. This is the first time that a gas core reactor has been operated at a power level sufficient to supply its own heat for maintaining the core in the vapor state. Operation in this mode was possible for only short periods of a few minutes duration This was not because of any problem with heat removal from the core, but was due to the necessity of keeping the inlet fuel line hot to prevent fuel migration to the cooled line which is normally heated by the air circulated from the external heaters to the core heating plenum

A summary of critical masses and fuel worths is given in Table 9.1 The deduced penalties of hydrogen and stainless were 11 0%Δk and 15 3%Δk respectively, and these values probably will be generally applicable to any similar configuration regardless of the base fuel density Figure 9 2 is a comparison of fuel worth results in this configuration vs that in the previous cylindrical configuration (Ref 1 through 5) As can be seen, the curve shapes are quite similar, indicating a rather general applicability of these results to any nominally similar reactor configuration The penalty one must pay in fuel loading to overcome a negative reactivity effect (such as increased hydrogen or wall thickness) becomes quite severe as the loading density increases

Fine radial power profiles were obtained, with catcher foils, on each of the three configurations tested Figure 9 3 shows the relative radial power distribution in the sensor well for all three configurations plotted on the same scale for easy comparison This data has been normalized to a relative power of one at the center of the core Likewise, the thermal flux calculated from thin bare and cadmium covered gold foils exposed in the sensor well, and from which infinitely dilute cadmium ratios were calculated, are plotted on the same scale for each of the configurations, in Figure 9 4 No unexpected surprises or anomalies were encountered in the detail of these power and flux maps

The neutron energy spectra as measured using a multiplicity of resonance and threshold detectors (See 6 2 2) are compared in Figures 9 5, 9 6, and 9 7 with the calculated spectra from the 19-energy group transport calculations It should be re-iterated that the calculated result had about a 3% positive bias in k-effective due ostensibly to the incorrectness of the hydrogen scattering kernel However, the energy spectra should only be affected within or very near to this very dilute hydrogen region by the scattering kernel used Comparison of these three figures shows that the slowing down flux is not flat in lethargy and differs in slope in various parts of the reactor Thus the flux is generally not asymptotic, and this condition stresses the need for the relatively fine energy group detail needed within the slowing down region The same comments can be applied to the thermal region even though such detail is not apparent in the figures

The worth of polyethylene in the void has been measured on a number of configurations, both in cylindrical and spherical geometries Results have varied from 0 17%Δk/kg to 0 6%Δk/kg of $CH_2$ On some configurations there was a strong worth dependence on radial position, with the higher worth being nearest the core The reverse appears to be true on this latest configuration, though the perturbing influence of the steel bolts on the upper core flange may have significantly influenced the measured results Furthermore, the trend on the previous cylindrical configurations was for lower specific polyethylene worth as the core fuel loading increased Again, on this recent spherical configuration, the reverse appears to be the case, though the conclusion must be labeled questionable because of the presence of the steel bolts The overall penalty of the $1x10^{21}$ H/cc in the form of both polyethylene and

TABLE 9 1

Summary of Critical Masses and Fuel Worth

for Three Configurations

| Configuration | Critical Core Loading (adjusted for K-excess and inlet line worth) | Fuel Worth %Δk/k per kg 93 2% enriched U-235 |
|---|---|---|
| #1 Clean Spherical Geometry | 8 43 | 2 96 |
| #2 1 x $10^{21}$ atoms/cc hydrogen added to cavity as CH & $CH_2$ | 12 9 | 2 02 |
| #3 0 0762 cm of stainless steel added to outer cavity wall | 29 2 | 0 437 |

polystyrene was 11 0%Δk, which reduces to an equivalent polyethylene worth of 0 42%Δk/kg assuming only the hydrogen contributes This further assumes equivalence of hydrogen worth in the CH and $CH_2$ molecules, a fact found to be true in one configuration (Ref 5, p 38) but not in another (Ref 3, p 88) Hence, the worth of hydrogen in the void has given varied results, with ostensibly no uniform trend pertaining to other reactor parameters The calculations of its effect have likewise not met with uniform success, particularly on calculating the penalty in fuel loading between Configurations 1 to 2 of this spherical experiment Hydrogen thus seems to present the major difficulty for this benchmark experiment, and this likely will also apply to operating cavity reactor calculations where high hydrogen temperatures will further complicate the problem

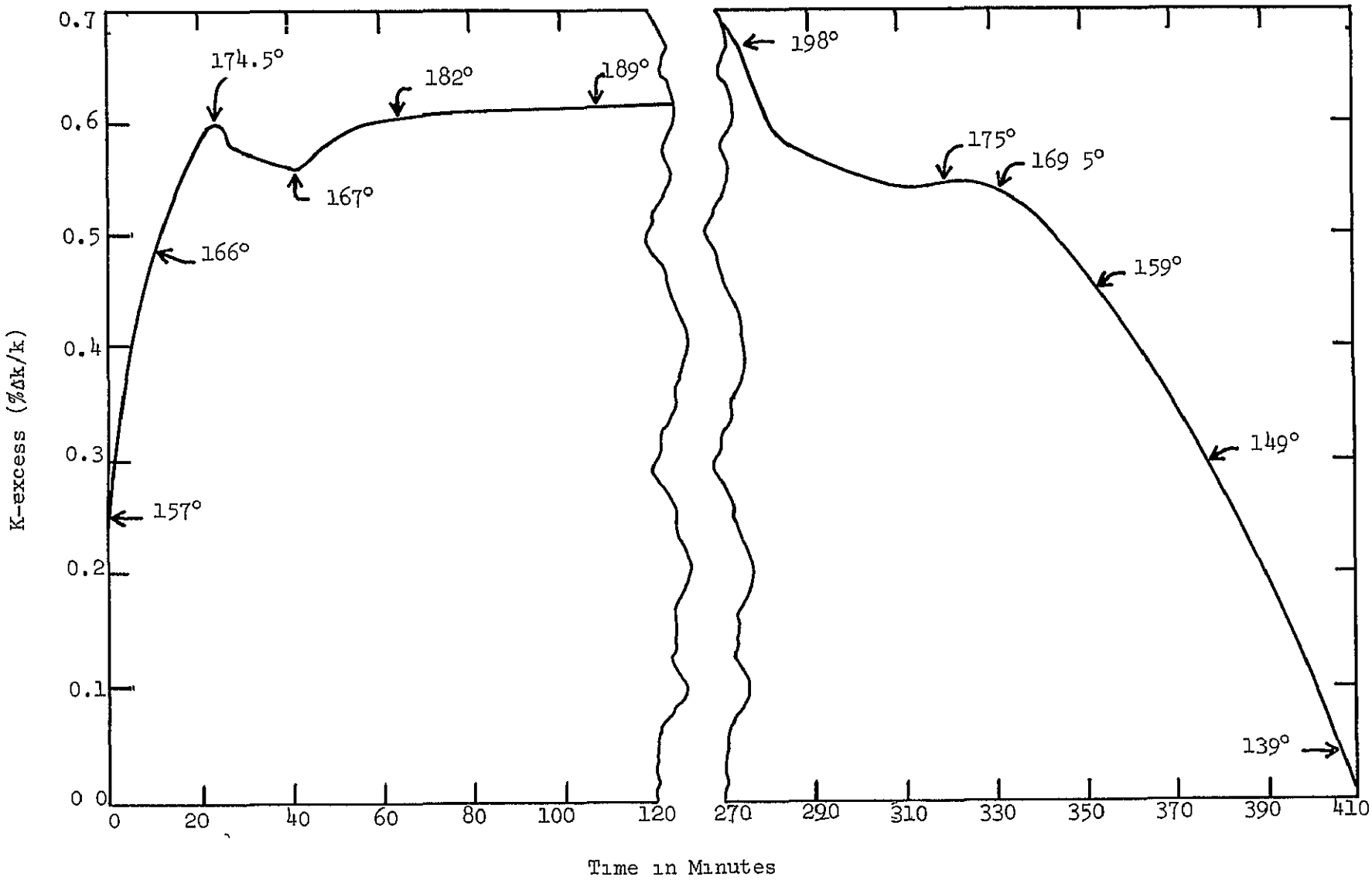


Figure 9 1 Reactivity changes during heatup and cooldown

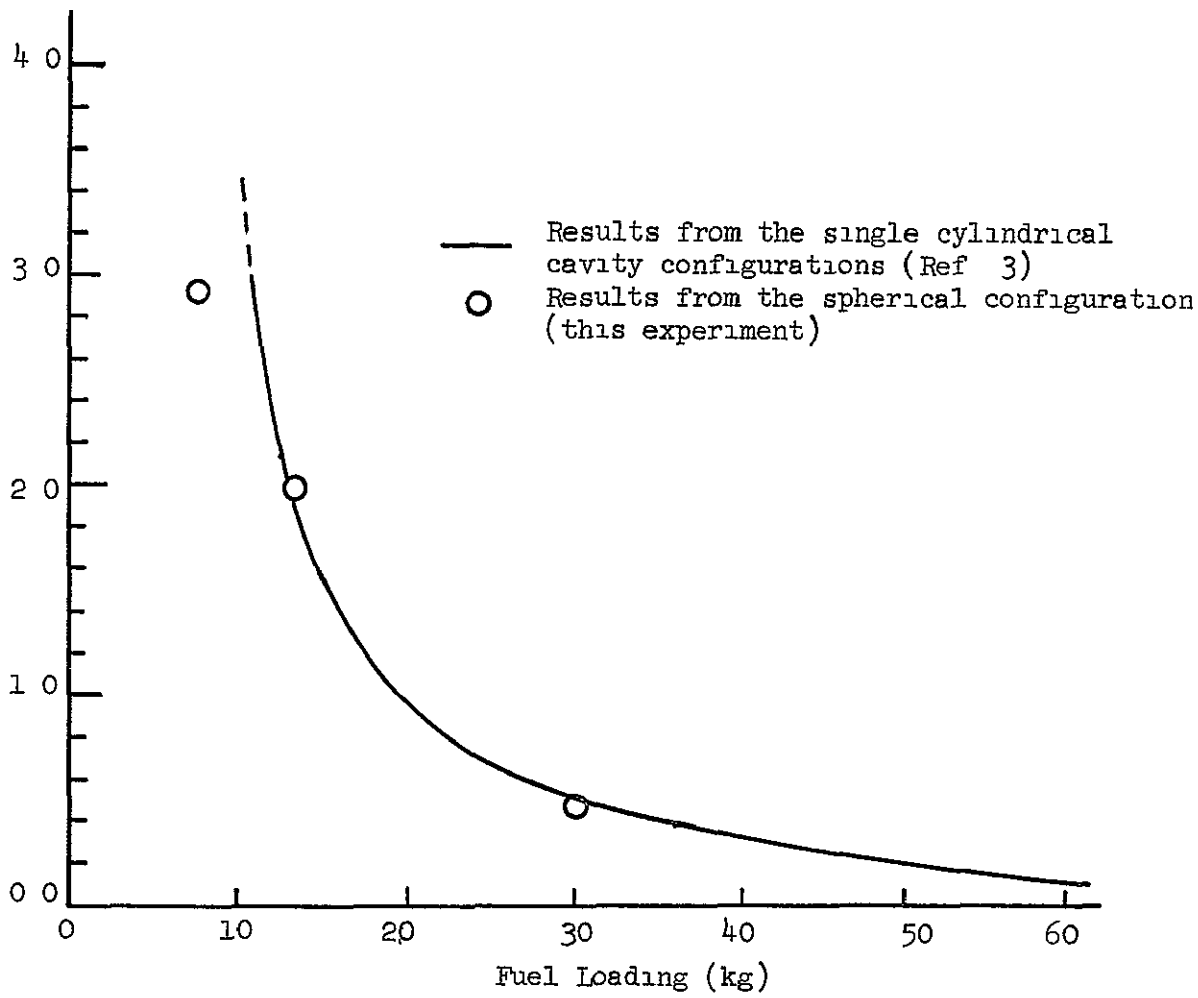


Figure 9.2 Comparison of Fuel Worth vs Fuel Loading for Two Configurations

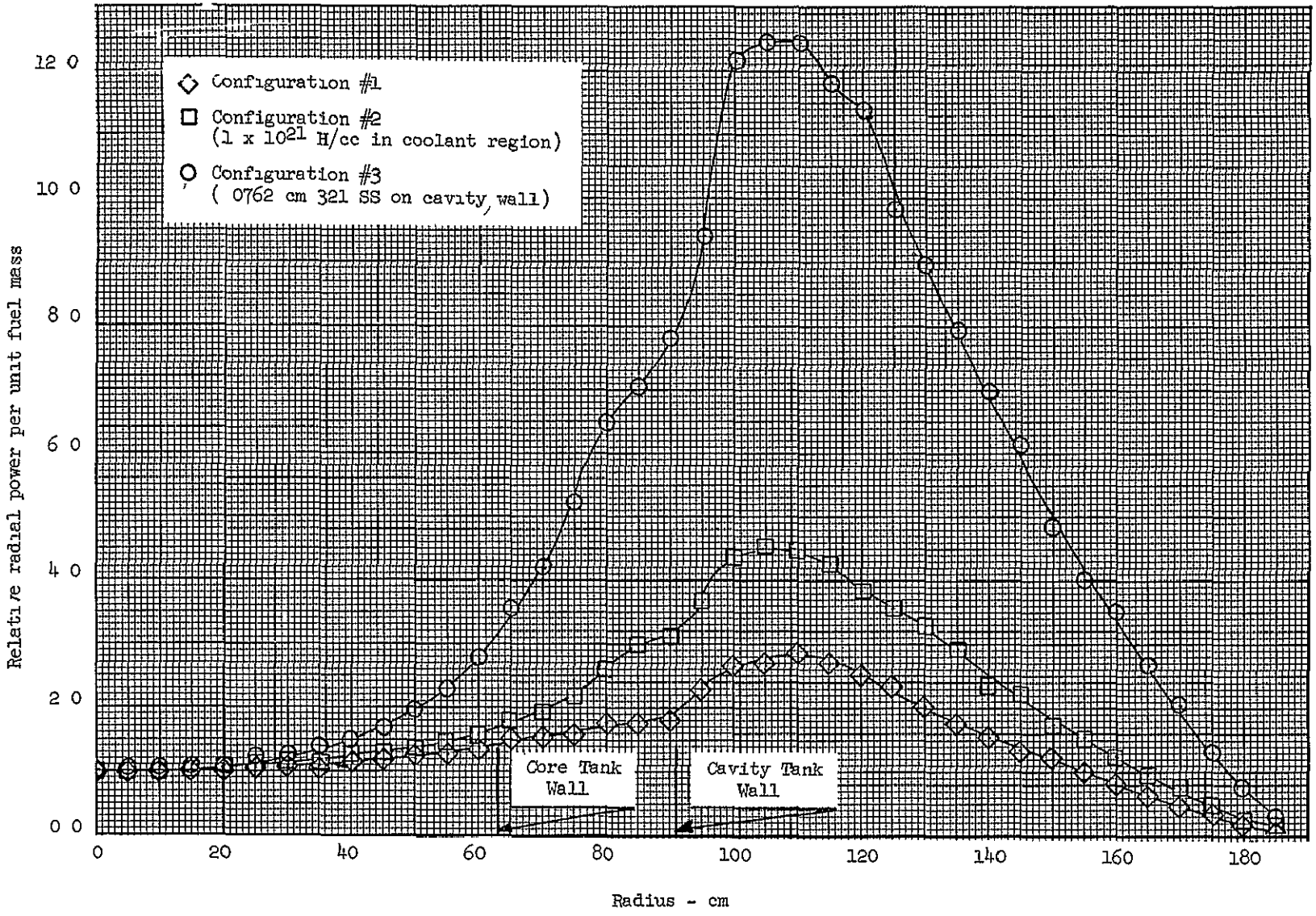


Fig 9 3 Comparison of relative radial fission rate for three Spherical Cavity Reactor Configurations

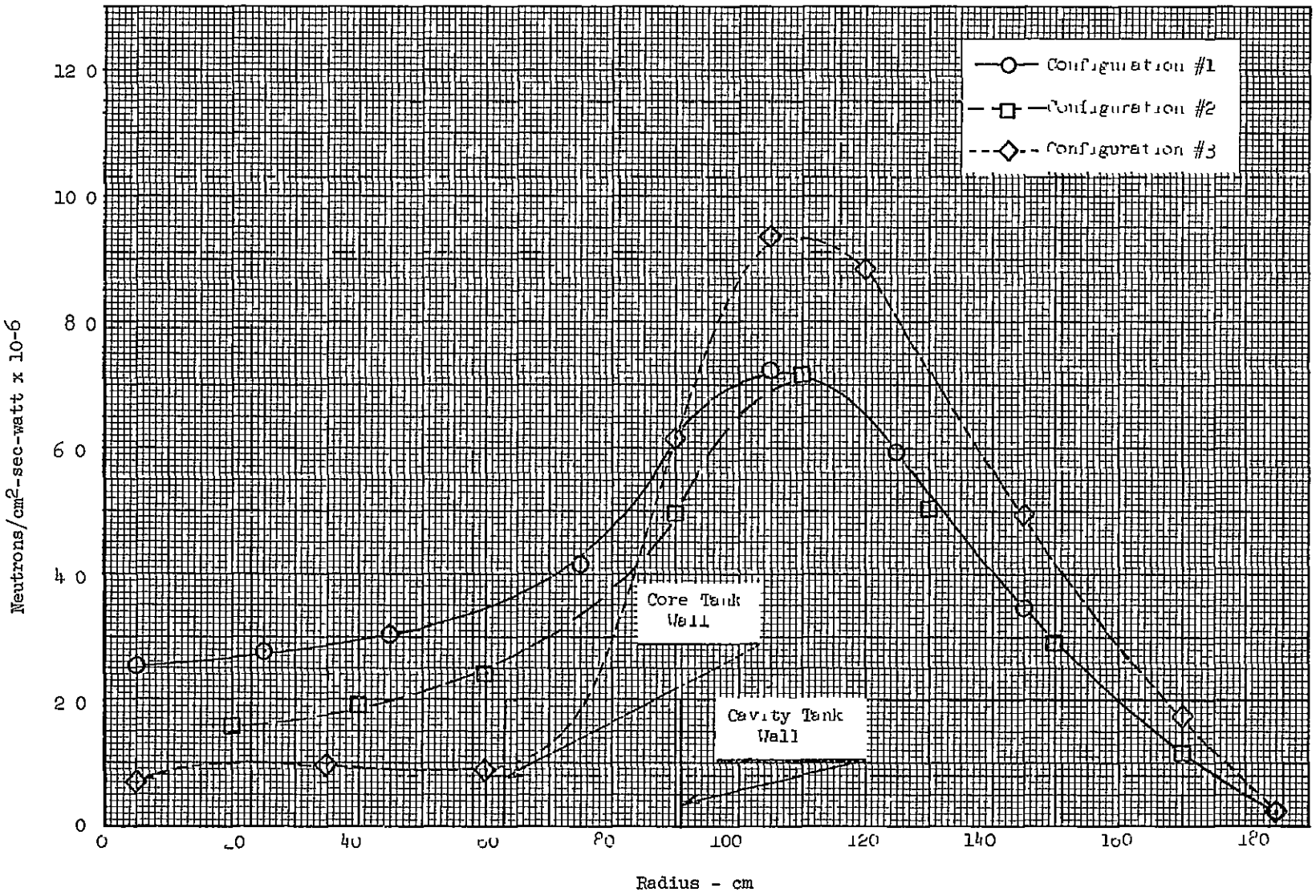


Figure 9 4 Thermal neutron flux determined from bare and cadmium covered gold foils in the sensor well for three configurations

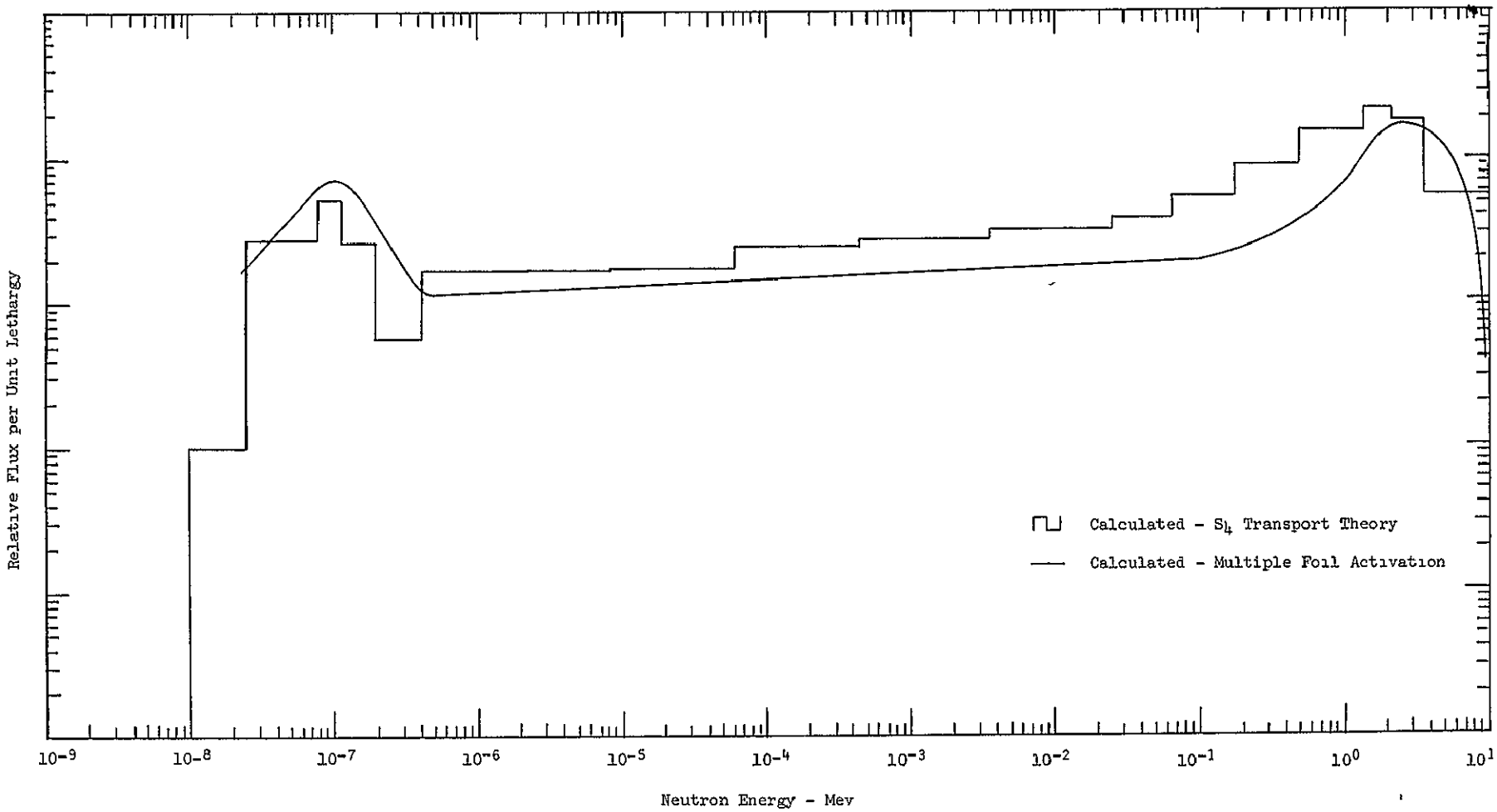


Fig 9 5 Comparison of neutron spectra calculated from multiple foil exposure and calculated with $S_4$, 19 energy group, transport theory (SCAMP code) at a radial distance of 0 0 cm

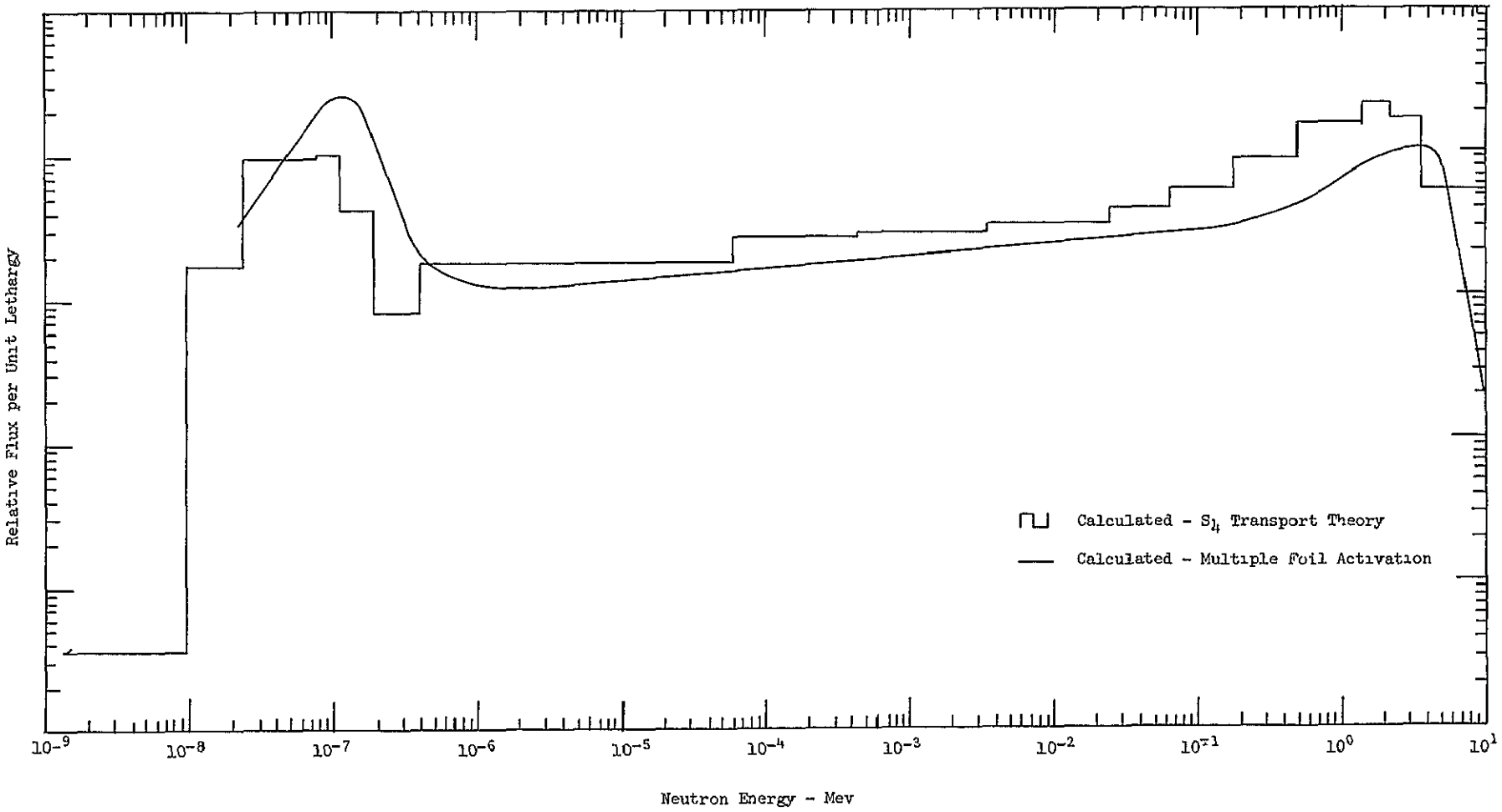


Fig 9 6 Comparison of neutron spectra calculated from multiple foil exposure and calculated with $S_4$, 19 energy group, transport theory (SCAMP code) at a radial distance of 61 0 cm

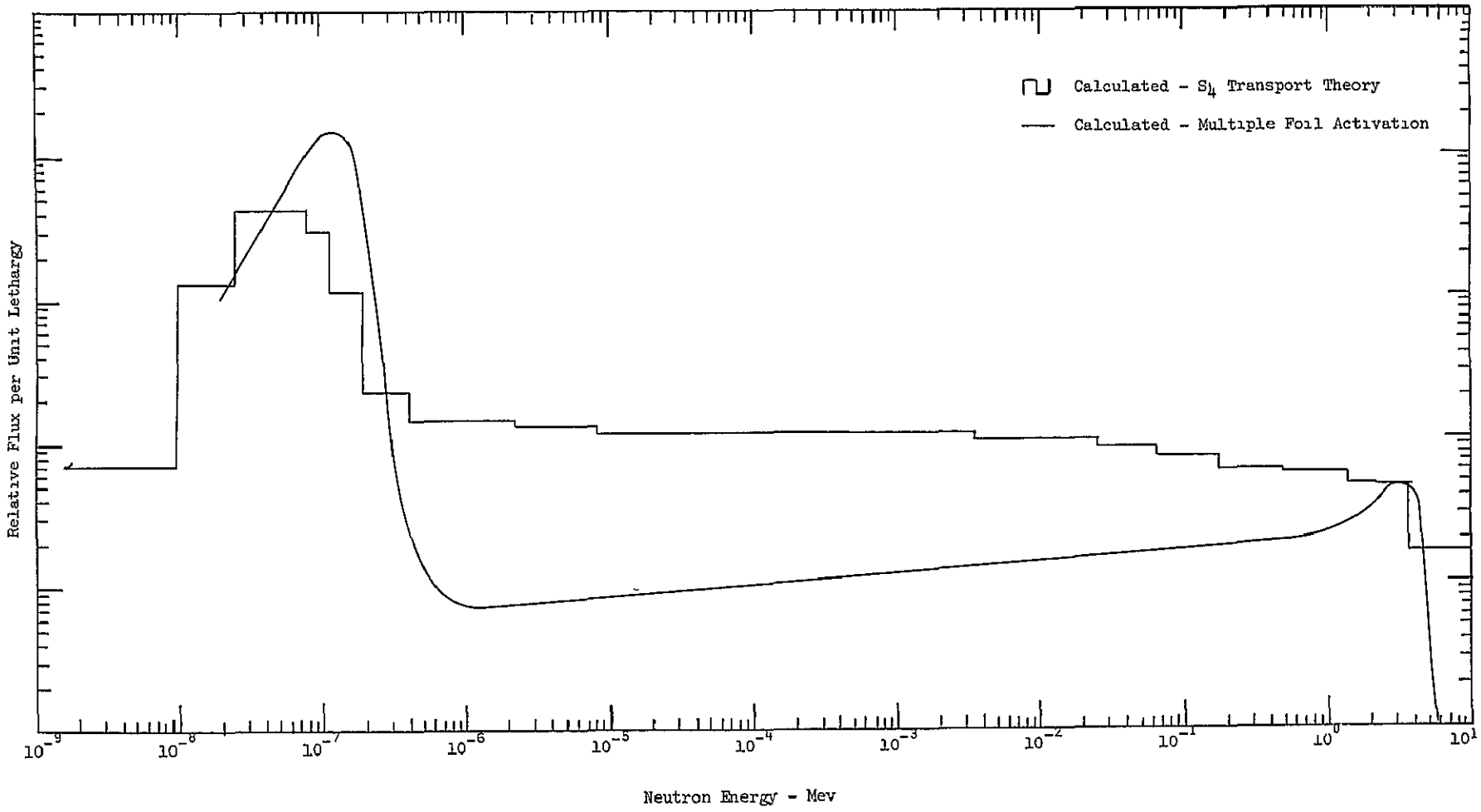


Fig 9 7 Comparison of neutron spectra calculated from multiple foil exposure and calculated with $S_4$, 19 energy group, transport theory (SCAMP code) at a radial distance of 105 0 cm

## 10 0 CONCLUSIONS AND RECOMMENDATIONS

1 The spherical symmetry with non-spherical perturbations being worth less than 1%$\Delta k$ makes this an ideal benchmark experiment for comparison with one dimensional spherical calculations

2 The penalty for hydrogen and neutron absorbing cavity walls is just as severe as in previous experiments, despite the relatively clean reflector in these latter configurations Hydrogen with a density of 1 x $10^{21}$/cc in the "void" raised the critical mass from 8 43 to 12 9 kg Then 0 076 cm extra thickness of stainless steel on the cavity wall (0 019 mean free absorption paths) raised the critical mass to 29 2 kg

3 Calculational difficulties exist with hydrogen (appears as a major effect on k-effective) and with the fuel (fuel worth incorrectly predicted) Since the temperature of these materials will change drastically between this cold experiment and operating gas-core reactor conditions, these two materials represent major reactor physics problems

4 Control methods and control adequacy for system reactivity does not appear to be a problem Very large amounts of reactivity can be controlled with several different schemes

5 As a result of these experiments, it appears that the next appropriate developmental step, that of a flowing gas critical experiment can be undertaken safely with respect to criticality control

## APPENDIX A

### Calculation of Infinitely Dilute Cadmium Ratios from Resonance Foil Activities

The following procedure was used to correct bare and cadmium covered resonance foil activities for self shielding and give cadmium ratios and thermal flux based on infinitely dilute foils. A single level resonance formula was employed as follows

$$A = B\left(\frac{I_\infty}{I_{eff}}\right) \text{ where} \left(\frac{I_\infty}{I_{eff}}\right) = \frac{1}{\sqrt{\dfrac{S/4NV}{S/4nv+\sigma_o(\Gamma\gamma/\Gamma)}}}$$

In terms of the foil radius and weight this reduces to

$$A = \frac{B}{\sqrt{\dfrac{\pi R^2\rho}{\pi R^2\rho+2NW\sigma_o(\Gamma\gamma/\Gamma)}}}$$

where

$A$ = Infinitely dilute cadmium covered foil activity per gram

$B$ = Uncorrected cadmium covered foil activity in activity per gram

$R^2$= Foil radius in cm

$\rho$ = Foil density in grams/cm$^3$

$N$ = Number of absorbing atoms/cm$^3$

$W$ = Cadmium covered foil weight

$\sigma_o$= Theoretical peak cross section of resonance

$\Gamma\gamma$= Gamma width

$\Gamma$ = Total width ($\Gamma\gamma+\Gamma n$)

$I_\infty$= Infinitely dilute resonance integral

$I_{eff}$= Effective resonance integral

$S$ = Foil surface area

$V$ = Foil volume

The sub-cadmium foil activity was determined as follows

$$S_a = C\text{-}A \Big/ \frac{I_\infty}{I_{eff}(\text{bare foil})}$$

where

$S_a$ = Subcadmium foil activity per gram at reactor shutdown

C = Bare foil activity per gram at reactor shutdown

A, $I_\infty$ and $I_{eff}$ are defined for the previous equation

This expression reduces to the following equation

$$S_a = C\text{-}A\sqrt{\frac{\pi R^2\rho}{\pi R^2\rho=2NW}}$$

where the expression under the square root sign is for the bare foil.

The thermal flux is then calculated from

$$S_a = \Sigma_a\phi V(1-e^{-\lambda t})$$

where

$\Sigma_a$= Macroscopic absorption cross section

$\phi$ = Neutron flux

V = Volume of 1 gram foil weight

$\lambda$ = Radioactive decay constant

t = Foil exposure time in the reactor

REFERENCES


1 Pincock, G D , Kunze, J F , "Cavity Reactor Critical Experiment, Volume I," General Electric Company, NMPO-ITS, September 6, 1967 (NASA-CR-72234).

2 Pincock, G. D., Kunze, J F., "Cavity Reactor Critical Experiment, Volume II," General Electric Company, NSP-ITS, May 31, 1968, (NASA-CR-72415)

3. Pincock, G. D , Kunze, J F , "Cavity Reactor Critical Experiment, Volume III," General Electric Company, NSP-ITS, September, 1968, (NASA-CR-72384)

4. Pincock, G. D , Kunze, J F , "Cavity Reactor Critical Experiment, Volume IV," Idaho Nuclear Corporation, October, 1969, IN-1336 (NASA-CR-72550)

5. Pincock, G D., Chase, P L , "Cavity Reactor Critical Experiment, Volume V," Idaho Nuclear Corporation, November, 1969, IN-1340 (NASA-CR-72577)

6. Henderson, W B , Kunze, J F , "Analysis of Cavity Reactor Experiments," General Electric Company, NSP-ITS, January, 1969 (NASA-CR-72484)

7 Lanzo, D. C , "A Flow Experiment on a Curved-Porous-Wall Gas-Core Reactor Geometry," Nuclear Applications and Technology, Vol. 8, No 1, page 6, January 1970

8 Kelber, C N., "Resonance Integrals for Gold and Indium Foils", Nucleonics, August, 1962, p 162

9. Dalton, G R and Osborne, R K , "Flux Perturbations by Thermal Neutron Detectors", Nuclear Science and Engineering, Vol 9, p 198 February, 1961

10. Brown, H. L and Connolly, T J , "Cadmium Cutoff Energies", Nuclear Science and Engineering, Volume 24, p 6, January, 1966

11. Private Communication, Letter C L Beck to R S Marsden "Input Description of SCAMP Codes ($S_n$ Codes for the Analysis of Multigroup Problems)" January 19, 1968

12. Masters, C. F., Cady, K B , "A Procedure for Evaluating Modified Pulsed-Neutron-Source Experiments in Subcritical Nuclear Reactors," Nuclear Science and Engineering, Volume 29, No 2, August, 1967

13. Simmons, B E., King, J S , "A Pulsed Neutron Technique for Reactivity Determination," Nuclear Science and Engineering, Volume 3, page 595, 1958

REFERENCES (Continued)


14 Idaho Nuclear Corporation Computer Code, Author G E. Putnam Reference letter Put-5-70, Aug 7, 1970, SCAMP Consolidation and Modification

15. "PHROG - a Fortran IV program to Generate Fast Neutron Spectra and Average Multigroup Constants" by R L Curtis, F J Wheeler, R A Grimesey, G L Singer (to be published)

16 "INCITE - A Fortran IV program to Generate Thermal Neutron Spectra and Multigroup Constants Using Arbitrary Scattering Kernels" by R L Curtis and R A Grimesey, November, 1967

17 Herwig, L O and Latham, T. S , "Nuclear Characteristics of Large Reflector-Moderated Gaseous-Fueled Cavity Reactors Containing Hot Hydrogen", American Institute of Aeronautics and Astronautics, Volume 5, No 5, pp 930-937, May 1967

INDEX

Aluminum, worth - 13, 14
Analytical, Correlation - 54, 55
Benchmark - 1, 67
Catcher foils - 5, 14, 20, 30, 36, 38, 58
Cavity tank - 3, 6, 7
Configurations -
    #1 - 1, 2, 12, 62, 63
    #2 - 1, 2, 28, 62, 63
    #3 - 1, 2, 35, 62, 63
Control -
    systems - 3, 12, 47
    methods - 1, 47, 48, 49, 67
    rod worth, curves, worth - 12, 19, 24, 53
Core tank - 3, 6, 7
Critical mass - 1, 59
Delayed neutrons -
    parameters - 4, 5, 9
Dimensions -
    reactor - 1, 3, 7, 8, 11
Deuterium ($D_2O$) - 3, 5, 47
Fuel ($UF_6$) - 2, 4, 5, 14, 28, 35, 42, 55, 57, 59, 61
Hydrogen, propellant - 1, 2, 35, 58, 67
Inverse multiplication - 17, 23
Mean Free Path (see stainless steel)
Multiplication factor, calculated - 1
Nuclear model - 16
Perturbations -
    from spherical - 1, 67
Polyethelene ($CH_2$) see configuration #2
    mass in cavity - 28
    worth - 14, 28
Polystyrene (see configuration #2)
    mass in cavity - 28
    worth - 4, 28

Power distribution
    configuration #1 - 25
    configuration #2 - 29
    configuration #3 - 36
Pulsed neutron
    methods - 1, 47, 48, 49
Reactivity worths
    see aluminum
    see stainless steel
    see polyethelene
    see polystyrene
References - 70, 71
Reflector-moderator 3, (see Deuterium)
Resonance foils
    Gold - 5, 15, 21, 26, 29, 31, 33, 36, 39, 44
    Indium - 15, 22, 36, 40
    Manganese - 15, 22, 36, 41
Sensor well - 3, 14
Spectrum - 37, 46, 58, 64, 65, 66
Stainless steel
    mass on cavity wall - 1, 2
    reactivity worth - 13, 35, 58
Temperature coefficient - 5, 57
Thermal absorber
    (see stainless steel)
Thermal neutron flux - 5, 21, 22, 27, 31, 34, 39, 40, 41, 45
Transport theory - 1, 2, 54, 58, 64, 65, 66